Appendix G.

Drill cuttings and fluids dispersion modelling study
(APASA 2012)

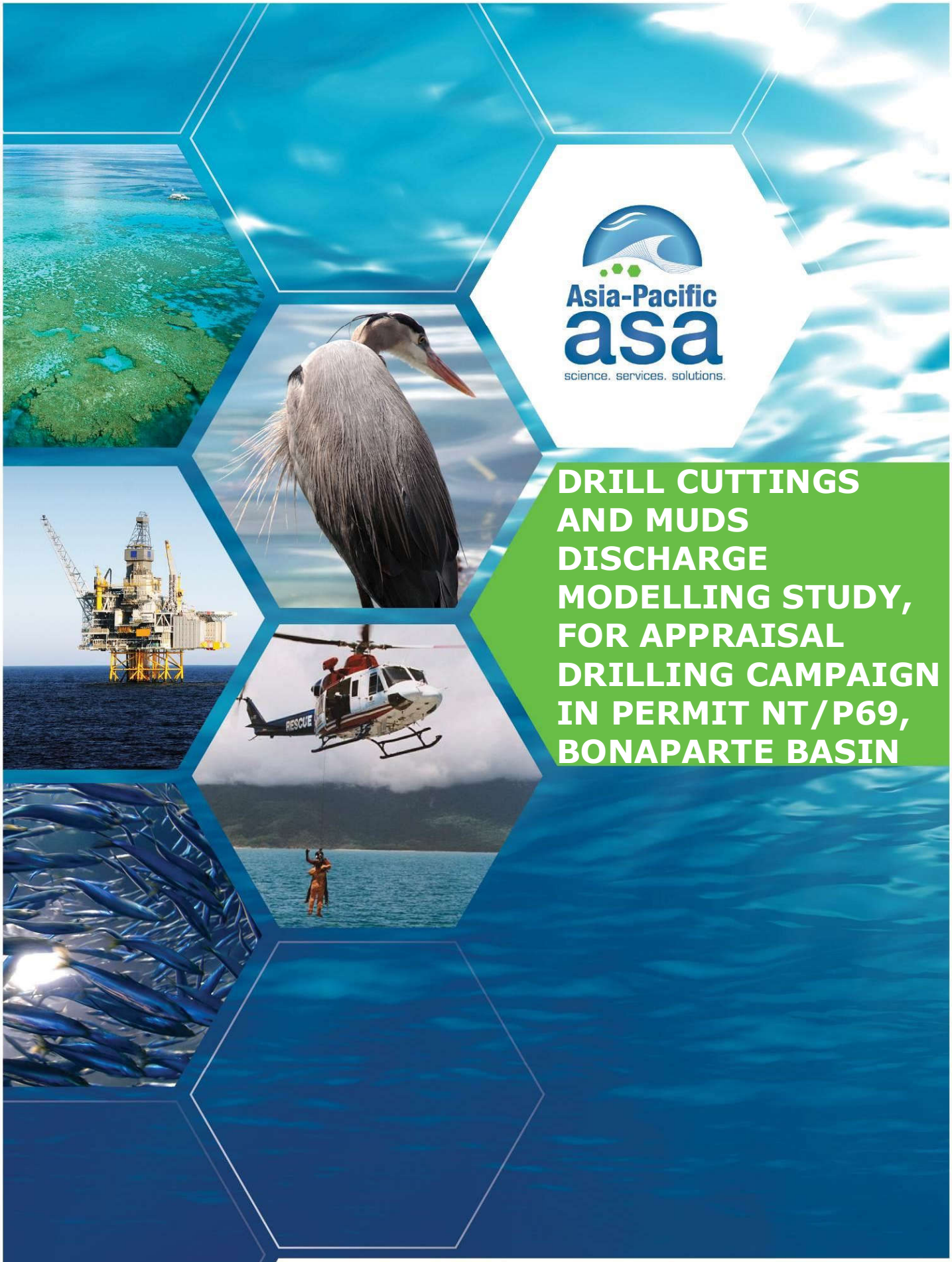

Asia-Pacific asa
science. services. solutions.

DRILL CUTTINGS AND MUDS DISCHARGE MODELLING STUDY, FOR APPRAISAL DRILLING CAMPAIGN IN PERMIT NT/P69, BONAPARTE BASIN

REV 1 - 13/12/2012

Prepared for:
ConocoPhillips Australia Pty Ltd

Document control form:

Revision	*Originated*	*Edit & review*	*Authorised*	*Date*
Rev A - Issued for internal review	*Alan Newnham* *Dr Sasha Zigic*	*Dr Sasha Zigic* *Dr Ryan Dunn*		
Rev 0 – Draft issued for client review		*Dr Sasha Zigic*	*Dr Sasha Zigic*	*25/06/2012*
Rev 1 - Issued for client review		*Dr Sasha Zigic* *Dr Ryan Dunn*	*Dr Sasha Zigic*	*13/12/2012*

Document name: COPA_Barossa-NTP69_Cuttings Modelling_Report_Rev1

APASA Project Number: Q0086

APASA Project Manager: Dr Sasha Zigic

Contact Details:

Asia-Pacific Applied Science Associates

Physical Address: Suite 3, Level 8
8-10 Karp Court, Bundall
Gold Coast, QLD 4217

Postal Address: PO Box 1679
Surfers Paradise, QLD 4217

Telephone: (0)7 5574 1112

Facsimile: (0)7 5574 1113

DISCLAIMER:

Contents

Figures

Tables

EXECUTIVE SUMMARY

Background

ConocoPhillips Australia Exploration Pty Ltd (ConocoPhillips) intends to drill, evaluate and flow test up to three hydrocarbon appraisal wells (appraisal wells) in petroleum exploration permit NT/P69. This permit is located in the Bonaparte Basin, in Commonwealth waters offshore the Northern Territory (NT). The appraisal wells comprise the Bonaparte Basin Barossa Appraisal Drilling Campaign (the drilling campaign). The drilling campaign will seek to determine whether potentially commercial hydrocarbon resources exist within the Barossa gas field which was discovered in 2006.

Each well is to be drilled as four separate intervals (conductor, surface, intermediate and production hole), with the diameter of each section decreasing with increasing depth. The conductor and surface holes will be drilled as an open system (riserless) with the extracted drill cuttings and fluids returned directly to the seafloor from the wellhead over 10.9 days. The cuttings and used fluids from the intermediate and production holes will be brought up to the surface through a riser for treatment through solids control equipment and discharged overboard near the sea surface over 28.4 days (approximately). In total approximately 39.3 days of active drilling is anticipated to complete each well.

Prior to commencing the drilling campaign, a dispersion modelling study was conducted to estimate the spatial distribution of the discharged cuttings and fluid solids deposited on the seabed. The discharges were simulated for one release location. As a conservative approach the closest location in the drilling area to the shoals was selected as the proposed release site for the modelling study. Point “F” is located approximately 60 km from Evans Shoal and 70 km from Tassie Shoal.

The main objective of this study was to report the total predicted sediment deposition (g/m^2), resulting from the discharge of drill cuttings and fluid solids over 10.9 days (near seabed discharge – total model duration of 15 days) and 28.4 days (surface discharge – total model duration of 32 days), under varying current conditions for the start of each calendar month (January to December).

The modelling applied a minimum threshold of 10 g/m^2 total (non-temporal, total load), over the entire modelling period (i.e. total period of discharge); equating to an average sedimentation rate of 0.2 g/m^2/day.

Methodology

The modelling study was carried out in several stages. Firstly, the tidal currents for the region were generated using ASA's ocean/coastal model, HYDROMAP. Secondly, the large scale ocean currents were obtained from the CSIRO Bluelink ReANalysis (BRAN) ocean model for the same region over a one year period (2004) and combined with tidal currents. The year-long dataset describes the complex vertical (through the water column with respect to depth) and horizontal (across the water column with respect to distance) current patterns. Finally, the current data and discharge characteristics were used as input into the far-field sediment model, MUDMAP, to predict the movement and initial settlement of discharged drill cuttings and fluids for the start of each month.

The 2004 ocean current data was selected as it was shown to include periods where strong ocean currents were directed towards the nearby shoals providing a conservative approach to the modelling in regard to potential sediment deposition.

In addition, sediment re-suspension was not included as part of the study as in an oceanic, open water environment such as the drilling area, it would ultimately have a dilution effect (i.e. reduce the total deposition loading at any location) and that sediments would, over time, demonstrate a net migration away from the high energy shallow water environment of the reefs into the surrounding deeper, depositional areas. Consequently, the original sedimentation footprint as reported herein would likely represent a worst-case in terms of total deposition on the shoals environment, rather than an underestimation.

Results: Near-seabed discharges

During drilling of the initial well sections (conductor and surface intervals) where drill cuttings and fluids will be discharged to the seabed, modelling indicated that the larger sediments (diameter greater than 0.15 mm) would settle within 60 m south from the release site. The modelling also showed that sediments smaller than 0.15 mm diameter will be carried further away from the release site (up to 3-4 km), due to slower settling velocities, in varying directions as a very thin layer of sediments. Within 100 m from the release site, the average and maximum bottom thickness was 4.5 mm and 11 mm, respectively.

No sediments were predicted to make contact with Evans Shoal or Tassie Shoal at a measureable level (above a value of 0.0026 mm or 10 g/m^2). The minimum distance from Evans Shoal and Tassie Shoal to the 10 g/m^2 contour was 53.1 km and 62.0 km, respectively.

Results: Sea surface discharges

With the sea surface releases occuring approximately 220 m above the seabed, the sediment was exposed to the force of the current for a longer period of time, thus transporting the material further away from the release site and causing it to settle over a larger area as a thinner pile. The seabed accumulation was much less compared to the seabed discharges. Within 100 m from the release site, the average and maximum bottom thickness was 0.05 mm and 0.14 mm, respectively.

No sediments were predicted to make contact with Evans Shoal or Tassie Shoal at a measureable level (above a value of 0.0026mm or 10 g/m^2). The minimum distance from Evans Shoal and Tassie Shoal to the 10 g/m^2 contour was 60.2 km and 67.9 km, respectively,

1 INTRODUCTION

1.1 Project Background

ConocoPhillips Australia Exploration Pty Ltd (ConocoPhillips) intends to conduct an appraisal drilling campaign in permit NT/P69. This permit is located in the Bonaparte Basin, in Commonwealth waters offshore the Northern Territory (NT) (see Figure 1).

Each well is to be drilled as four separate intervals (conductor, surface, intermediate and production hole), with the diameter of each section decreasing with increasing depth. The conductor and surface holes will be drilled as an open system (riserless) with the extracted drill cuttings and fluids returned directly to the seafloor from the wellhead. The cuttings and used fluids from the intermediate and production holes will be brought up to the surface through a riser for treatment through solids control equipment and discharged overboard near the sea surface. Approximately, 39.3 days will be required to complete the active drilling of each well, with the discharge of drill cuttings and fluids near the seabed conducted over 10.9 days and the sea surface discharges over a 28.4 day period (approximately).

Prior to commencing the drilling campaign, a dispersion modelling study was conducted to estimate the spatial distribution of the discharged cuttings and fluids deposited on the seabed. The study examined the near seabed and surface discharges under varying current conditions for the start of each calendar month (January to December) from one release location.

A conservative approach has been used to estimate the likely probability of exposure to sedimentation to the submergent shoals and distant shorelines in the region. Point “F” in Figure 1, the closest location in the drilling area to the shoals was selected as the proposed release site for the modelling study. Point “F” is located approximately 60 km from Evans Shoal and 70 km from Tassie Shoal, in a water depth of approximately 220 m. Figure 1 and Table 1 provides a summary of the modelled release location and water depth.

The main objective of this study was to report the total predicted sediment deposition (g/m^2), resulting from the discharge of drill cuttings and fluids over 10.9 days (near seabed discharge – modelled for 10.9 days) and 28.4 days (surface discharge – modelled for 28.4 days), under varying current conditions for the start of each calendar month (January to December).

Table 1: Release location used as part of the drill cuttings and fluids dispersion modelling study.

Latitude	Longitude	Water depth (m)
9° 54' 55.1" S	130° 10' 4.4" E	~220

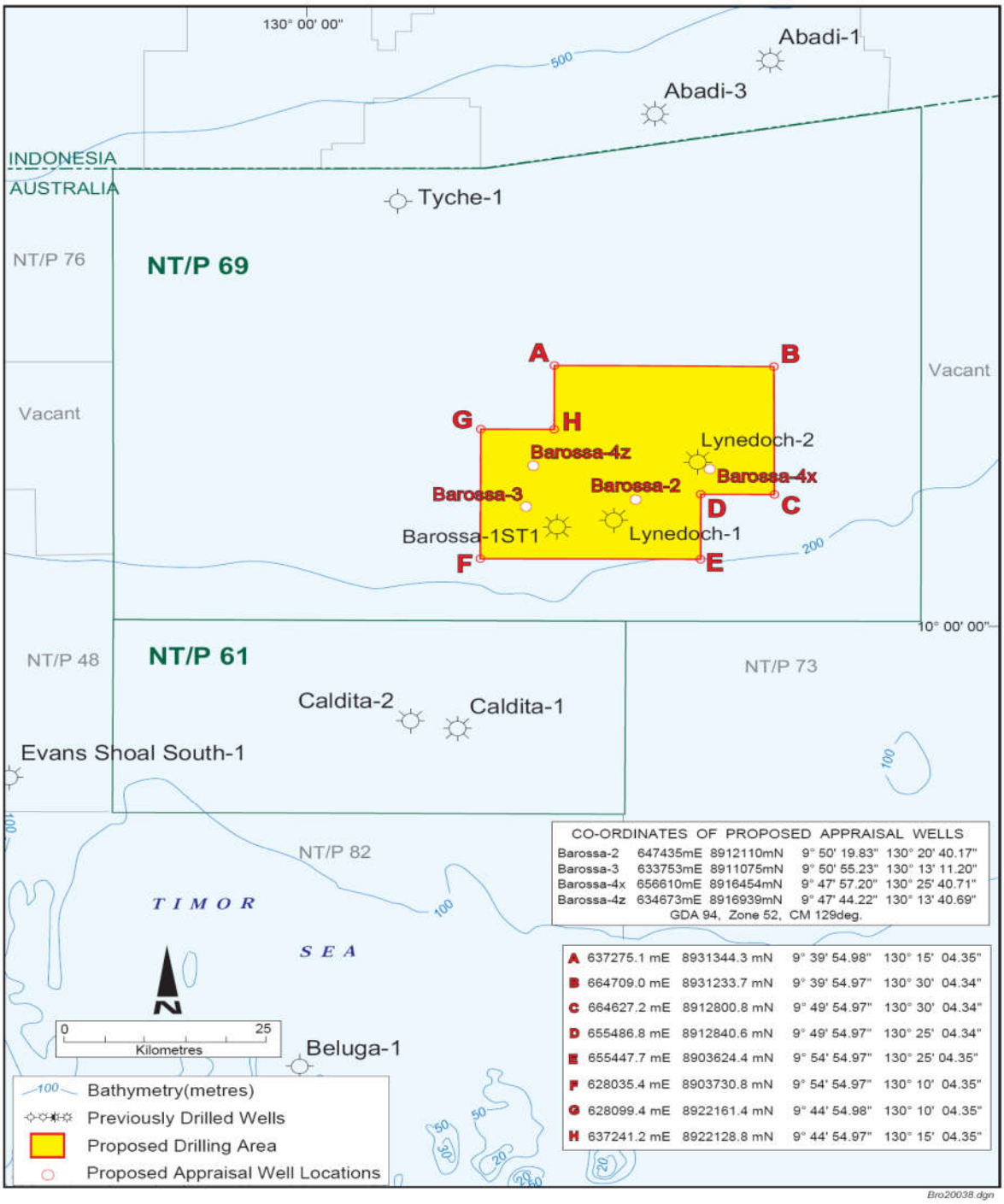

Figure 1: Map showing the location of the appraisal wells and release location in the drilling area, used as part of the drill cuttings and fluids dispersion modelling study. (source: ConocoPhillips Australia Exploration Pty Ltd July 2012).

1.2 Scope of Work

The scope of work included the following components:

1. Generate tidal current patterns of the receiving waters using a validated ocean/coastal model, HYDROMAP;
2. Create a year-long (2004) dataset describing the large scale flow of ocean waters from the CSIRO Bluelink ReANalysis (BRAN) ocean model and combine with HYDROMAP predicted tidal currents. This combined dataset was used to describe the total water current within the region;
3. Use current data and discharge characteristics as input into the far-field sediment model, MUDMAP, to predict the movement and initial settlement of discharged drill cuttings and fluids for the start of each month;
4. Report the predicted sediment deposition, area of coverage and distance from adjacent reefs, from the seabed discharge from the start of each month;
5. Report the predicted sediment deposition, area of coverage and distance from shoals and coastlines, from the surface discharge from the start of each month; and
6. Report the total predicted sediment deposition, area of coverage and distance from shoals and coastlines, from the combined seabed and sea surface discharge from the start of each month

2 REGIONAL CURRENTS

The drilling area is located within the influence of the Indonesian throughflow, a large scale current system characterised as a series of migrating gyres and connecting jets that are steered by the continental shelf. This results in sporadic events of deep ocean surface currents exceeding 1.5 m/s (~ 3 knots).

While the mass flow is generally towards the southwest, year-round, the internal gyres generate local currents in any direction. As these gyres migrate through the area, large spatial variations in the speed and direction of currents will occur at a given location over time.

While, the tidal currents are generally weak in the deeper waters, its influence is greatest along the inshore and coastal passage regions, and in and around, the many reef systems on the continental shelf. Hence, the net current forcing can be variably affected by the tidal and

deep ocean currents. Therefore it was critical to include the influence of both types of currents to rigorously understand the likely drift patterns of hydrocarbon spills within in the region.

2.1 Ocean Currents

To account for the prevailing ocean currents, data was obtained from the BRAN (Bluelink ReAnalysis – Oke et al., 2008, 2009; Schiller et al., 2008) model developed by CSIRO's Marine and Atmospheric Research group. It is a very comprehensive ocean current dataset, which includes data between October 1992 to December 2006. The model uses an assimilative technique for remotely sensed measurements and runs with a horizontal cell size resolution of approximately 10 km and 47 vertical layers.

For the study a five year data set was obtained (2001 to 2005 (inclusive)). Figure 2 shows the surface current roses for each individual year. Note the convention for defining current direction is the direction the current flows to, which is used to reference current direction throughout this report. Each branch of the rose represents the currents flowing to that direction, with north to the top of the diagram. Sixteen directions are used. The branches are divided into segments of different colours, which represent the current speed interval for each direction. Speed intervals of 0.1 m/s are used in these current roses. The length of each coloured segment is relative to the proportion of currents flowing within the corresponding speed and direction.

Figure 3 shows the seasonal surface current roses for 2004 as an example at the modelled release site. The data shows that the ocean current speeds and directions varied between seasons. During the winter (April to August) and transitional (March and September to November) periods, currents flowed predominantly to the west-southwest. For the summer months (December to February) surface currents flowed in both a westerly and easterly direction. The current speeds were weaker during summer in comparison to the winter and transitional seasons.

Figure 4 shows a screenshot of the predicted ocean currents at the surface during summer and winter conditions. The colouration of the individual vectors indicates current speed (m/s).

As the model neglects tidal forcing, tidal currents were independently generated and added to describe the net water movement (see Section 2.2 Tid).

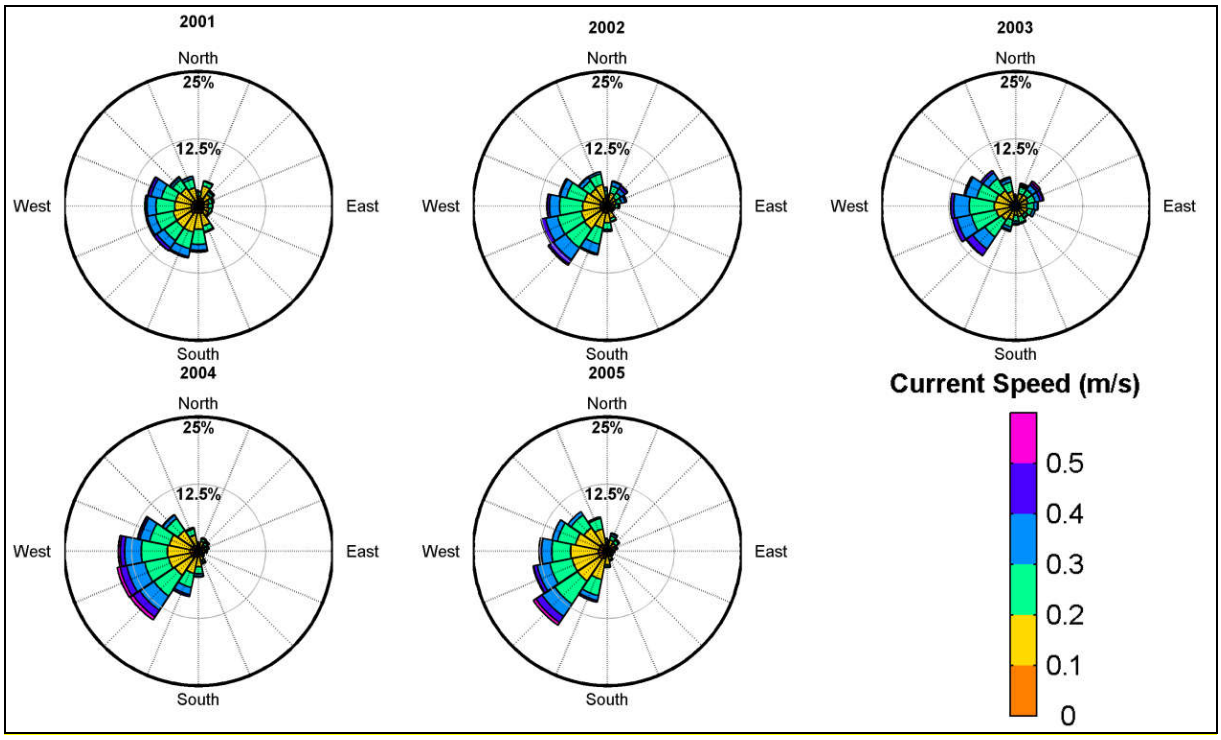

Figure 2: Annual surface ocean current rose plots at the modelled release location. Data from 2001 to 2005 was obtained from the BLUElink ReANalysis deep ocean model.

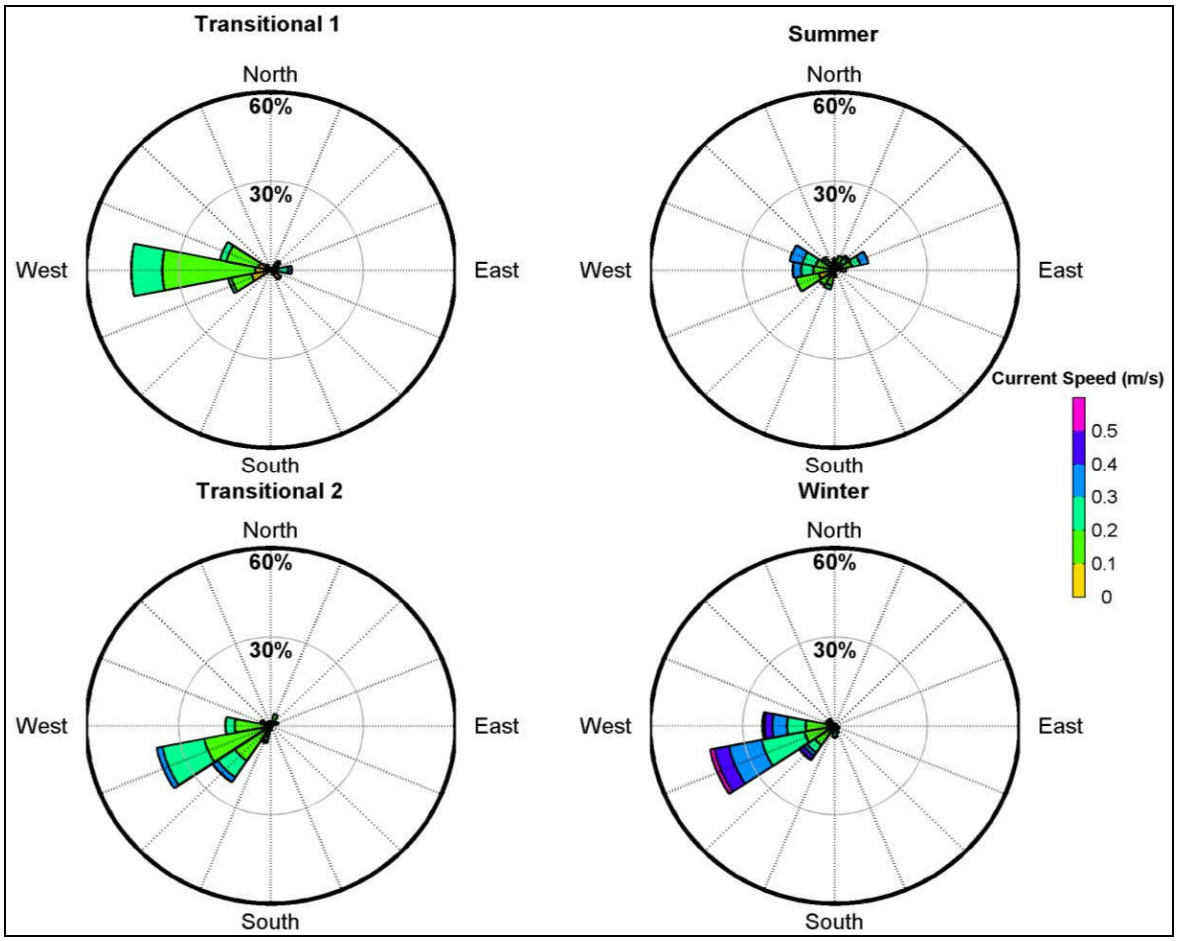

Figure 3: Seasonal current rose distributions for 2004 at the modelled release site.

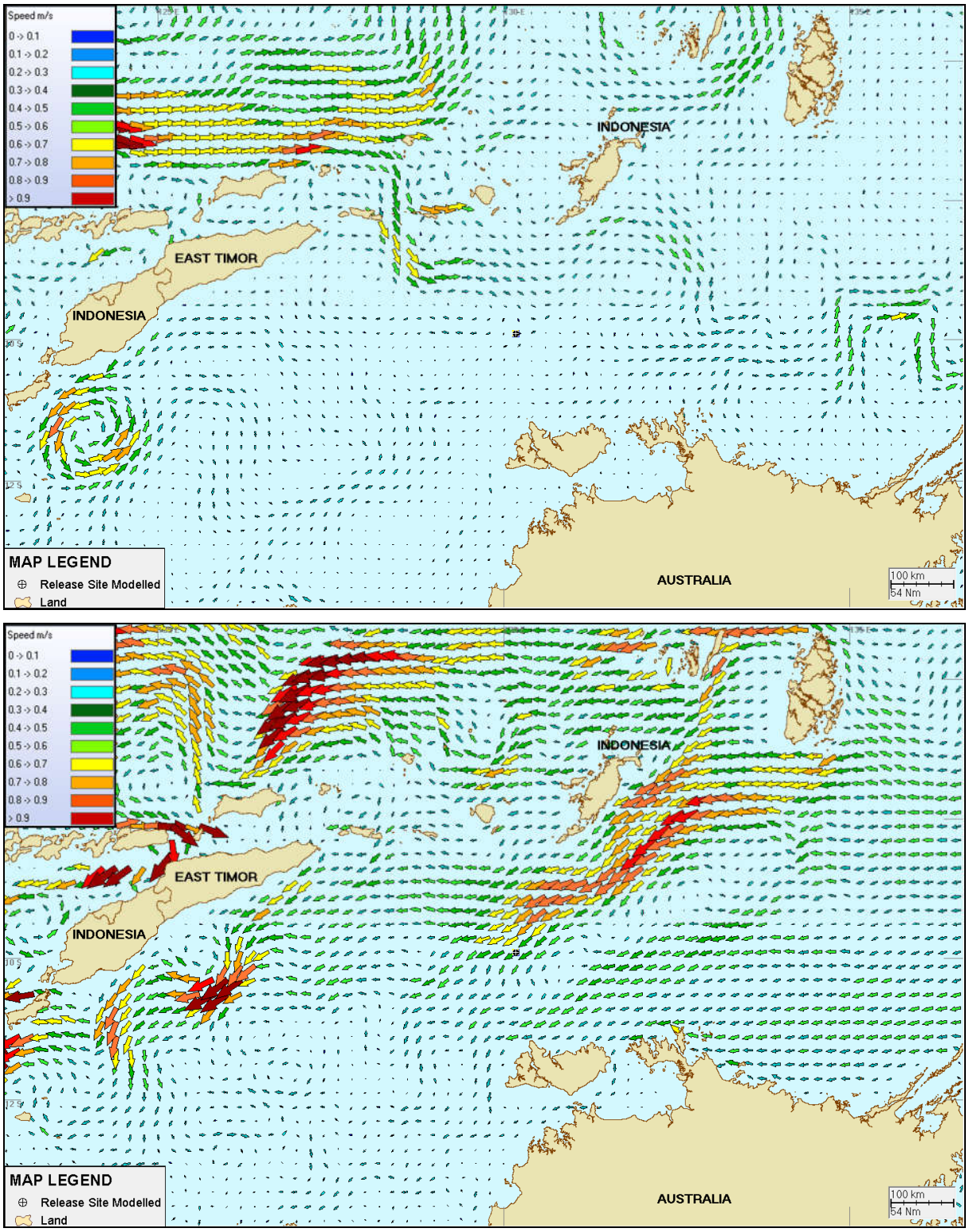

Figure 4: Screenshot of the predicted surface ocean current vectors during a single time-point during the summer (upper image) and winter seasons (lower image). The colours of the vectors indicate current speed in m/s. The release location is depicted by the black crosshair icon.

2.2 Tidal Currents

The tidal current data was generated using ASA's advanced ocean/coastal model, HYDROMAP. The HYDROMAP model has been thoroughly tested and verified through field measurements throughout the world over the past 25 years (Isaji and Spaulding, 1984; Isaji et al., 2001; Zigic et al., 2003). In fact, HYDROMAP tidal current data have been previously used as input to forecast (in the future) and hindcast (in the past) oil spills in Australian waters and forms part of the Australian National Oil Spill Emergency Response System operated by AMSA (Australian Maritime Safety Authority).

HYDROMAP simulates the flow of ocean currents within a model region due to forcing by astronomical tides, wind stress and bottom friction. The model employs a sophisticated nested-gridding strategy, supporting up to six levels of spatial resolution. This allows for a higher resolution of currents within areas of greater bathymetric and coastline complexity, or of particular interest to a study. To simulate the ocean-circulation over any area of interest, the model must be provided with the following data:

(1) Measured bathymetry for the area, which defined the shape of the seafloor;

(2) The amplitude and phase of tidal constituents, which were used to calculate sea heights over time at the open boundaries of the model domain. Changes in sea heights were used, in turn, to calculate the propagation of tidal currents through the model region; and

(3) Wind data to define the wind shear at the sea surface.

The numerical solution methodology follows that of Davies (1977a, 1977b) with further developments for model efficiency by Owen (1980) and Gordon (1982). A more detailed presentation of the model can be found in Isaji and Spaulding (1984).

1.1.1 Grid Set Up

HYDROMAP was set-up over a domain that extended 1,525 km (east–west) by 1,240 km (north–south). The domain was subdivided horizontally into a grid with 5 levels of resolution. The resolution of the primary level was set at 14 km. The resolution of the second, third, fourth and fifth levels were 7 km, 3.5 km, 1.75 km and 876 m, respectively. The finer grids were allocated in a step-wise fashion to more accurately resolve flows along the coastline, around islands and over more complex bathymetry.

1.1.2 Tidal Data

The detailed tidal data was in the form of amplitude and phase records along the open boundaries of the model grid, which was extracted from the Topex/Poseidon global tidal database (TPX07.1; National Oceanographic and Atmospheric Administration). The database is derived from long-term satellite measurements. Using the tidal data, surface heights were firstly calculated along the open boundaries, at each time step in the model, using the eight largest and most significant tidal constituents for the area (M_2, S_2, K_1, O_1, N_2, P_1, K_2, and Q_1).

For the purposes of verifying the tidal data, results from a 29-day simulation were compared against the National Tidal Facility (NTF) observed tides at six tide stations (Table 2). As can be seen in Figure 5 and Figure 6, the HYDROMAP predictions compare very well to the timing and height of the observed tidal data. This demonstrates that the model and input data is accurately predicting the propagation of tidal currents.

Table 2: Location of observation tide stations

Station	Latitude and Longitude	Distance to NT/P69 (km)
Newby Shoal	11° 52' S; 129 ° 11' E	230
Two Hills Bay	11° 31' S; 132 ° 4' E	240
Jensen Bay	11° 11' S; 136 ° 41' E	690
Sir Charles Hardy Island	11° 55' S; 143 ° 28' E	1,330
Archer River	13° 20' S; 141 ° 39' E	1,270
Port Moresby (Papua New Guinea)	9° 29' S; 147 ° 6' E	1,820

Figure 7 shows a screen shot of the predicted tidal current vectors surrounding the drilling area. Note, only every 3rd tidal vector is shown to ensure clarity. The colouration of the individual vectors in Figure 7 indicates current speed.

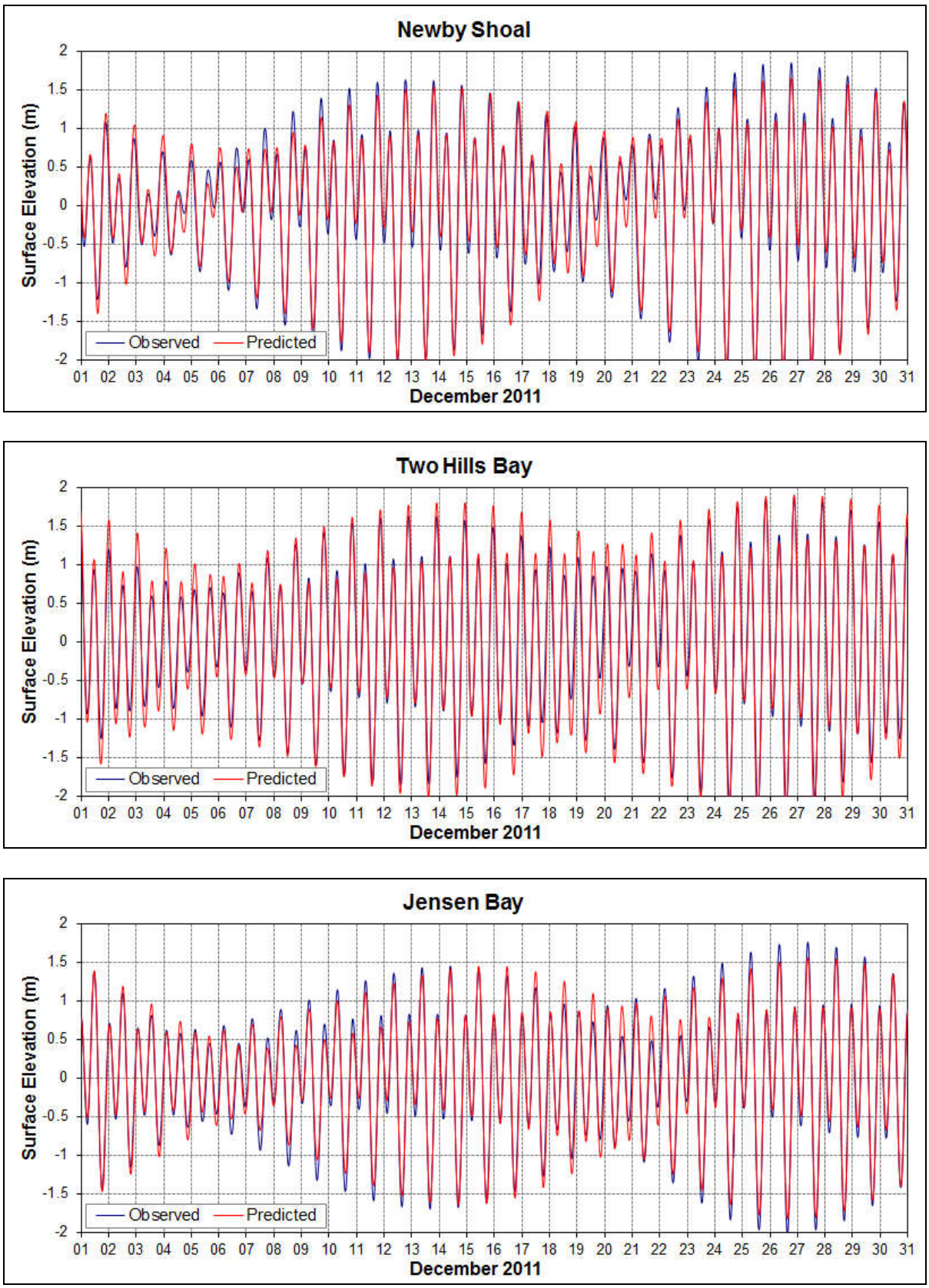

Figure 5: Comparison between predicted (red line) and observed (blue line) surface elevations at Newby Shoal (top), Two Hills Bay (middle) and Jensen Bay (bottom), 1st - 31st December 2011.

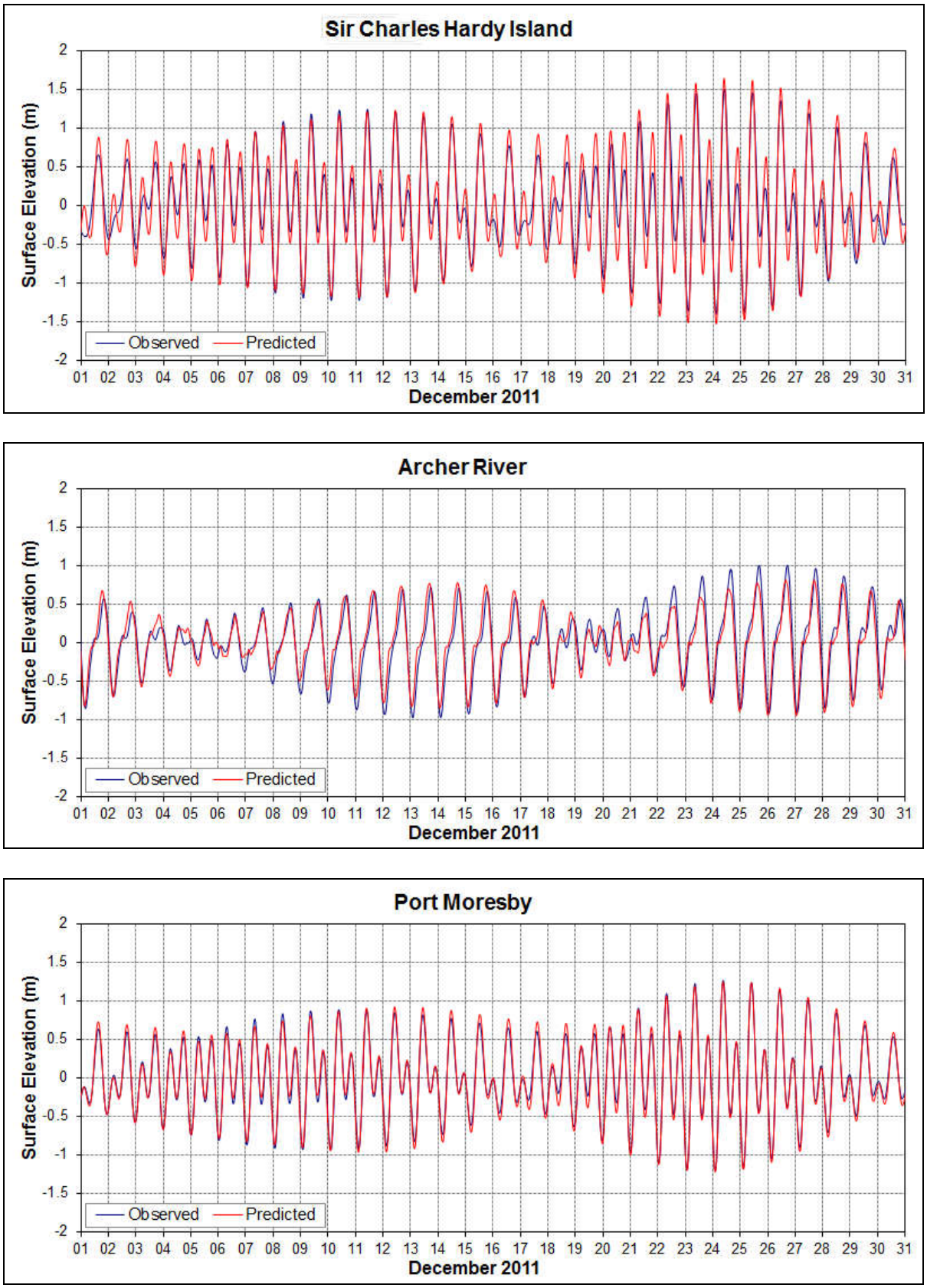

Figure 6: Comparison between predicted (red line) and observed (blue line) surface elevations at Sir Charles Hardy Island (top), Archer River (middle) and Port Moresby (bottom), 1st - 31st December 2011.

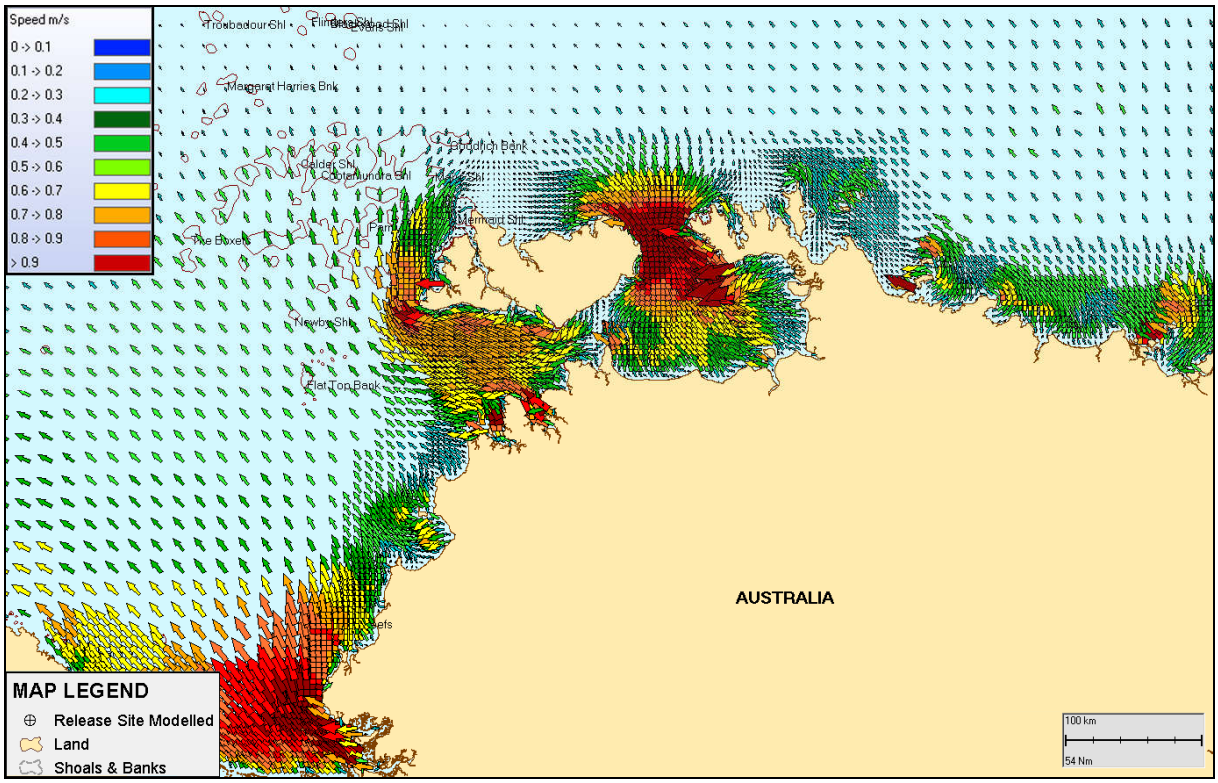

Figure 7: Screenshot of the predicted tidal current vectors. Note the density of the tidal vectors vary with the grid resolution, particularly along the coastline and around the islands. Colourations of individual vectors indicate current speed in m/s.

2.3 Net Water Current

Figure 8 show the monthly and annualised surface and near bottom current roses at the release location for 2004. Note the convention for defining current direction is the direction the current flows to, which is used to reference current direction throughout this report. Each branch of the rose represents the currents flowing to that direction, with north to the top of the diagram. Eight directions are used. The branches are divided into segments of different thicknesses, which represent current speed ranges for each direction. Speed intervals of 0.1 m/s are used in these current roses. The width of each segment within a branch is proportional to the frequency of currents flowing within the corresponding range of speeds for that direction (e.g. thick segments of the branches represent a higher frequency of currents of that speed flowing in that direction compared to segments which are thinner).

As the current roses illustrate, the speeds and directions vary as a function of depth. The average and maximum surface currents were 0.2 m/s and 0.71 m/s, respectively, which are significantly stronger than the near bottom currents (an average and maximum of 0.1 m/s and 0.4 m/s, respectively).

Directionality of the surface currents were also shown to vary between each month, predominately due to the prevailing seasonal wind conditions. During the summer months (December to the following February) the winds were from the west which is in opposite direction of the main current flow. While during the winter months (April to August), winds blew from the east, which in line with the direction of the currents.

Figure 9 shows the hourly predicted net surface current speeds and directions and Figure 10 shows the hourly predicted net bottom current speeds and directions for 2004 at the modelled release site.

As shown in Figure 9, compared to Figure 10, the surface current speeds were consistently higher for an extended period of time, due to the influence of winds.

Figure 11 is a screenshot of the predicted net surface and bottom current vectors surrounding the modelled release site, at 12 am 1st April 2004. The image again demonstrates the higher current speeds at the surface compared to the bottom waters. Note the difference in directionality between surface and bottom currents at the selected point in time.

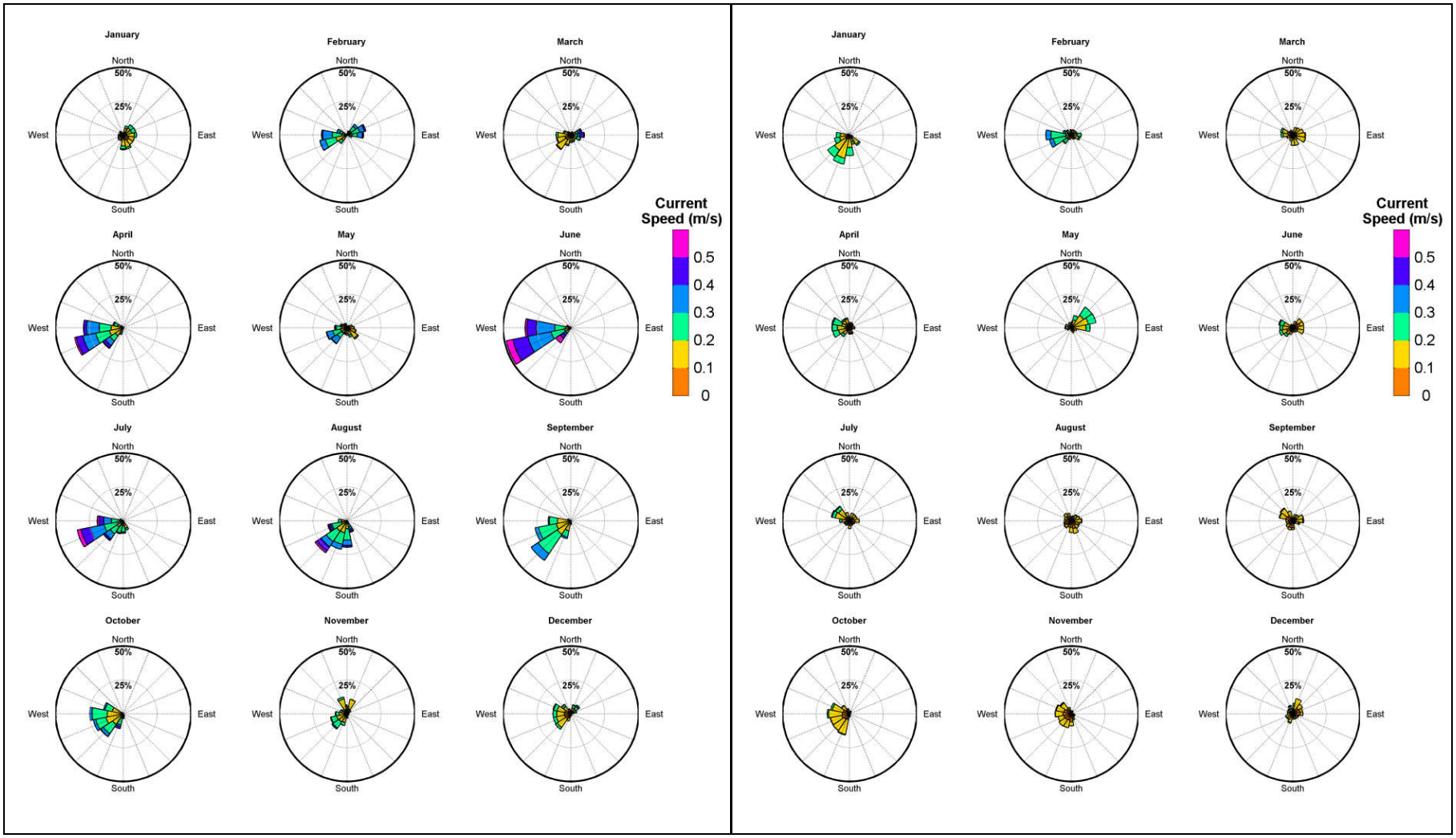

Figure 8: Monthly net surface (left image) and bottom (right image) current roses at the modelled release site for 2004. Current roses depict the net movement of currents (combined ocean and tidal currents).

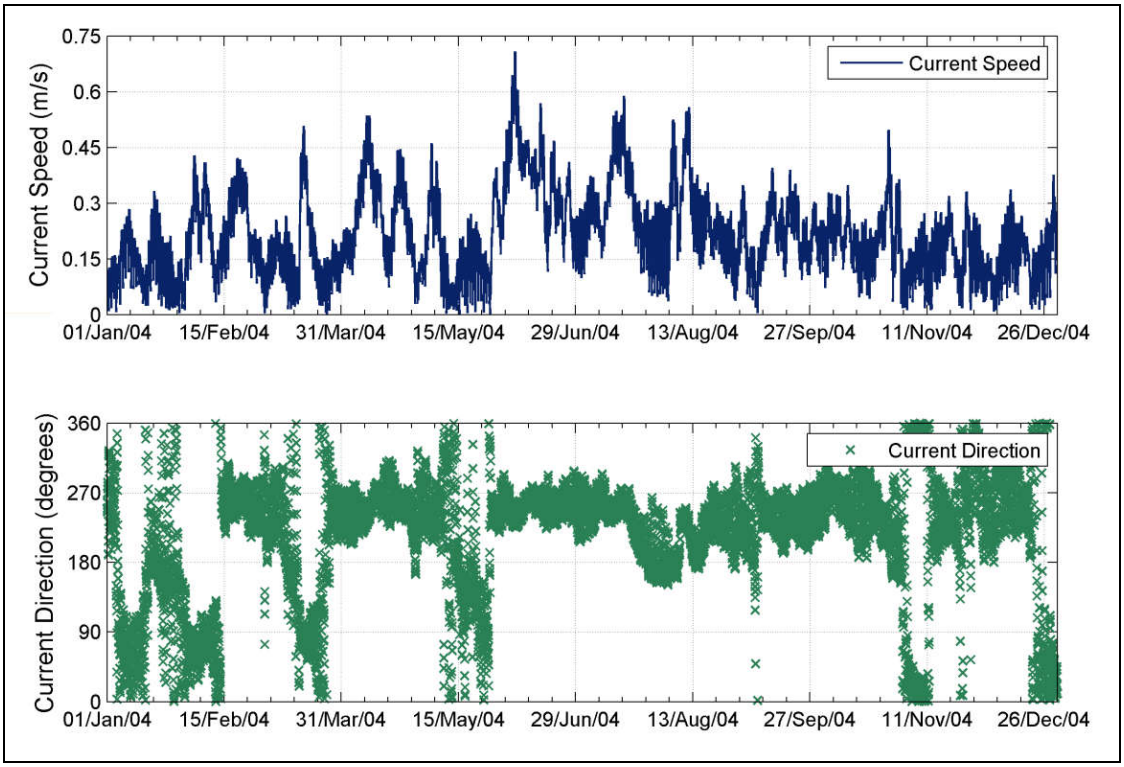

Figure 9: Predicted hourly net surface current speeds and directions at the modelled release site for 2004. Currents depict the net movement of currents (combined ocean and tidal currents).

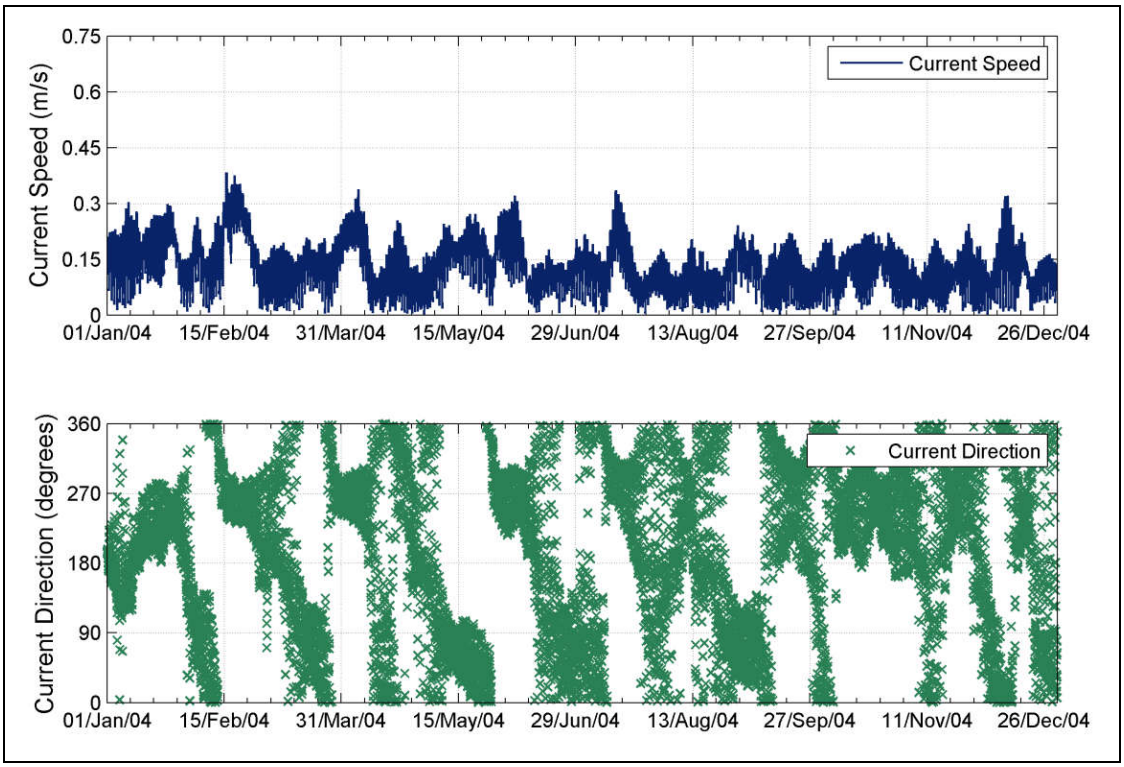

Figure 10: Predicted hourly net bottom current speeds and directions at the modelled release site for 2004. Currents depict the net movement of currents (combined ocean and tidal currents).

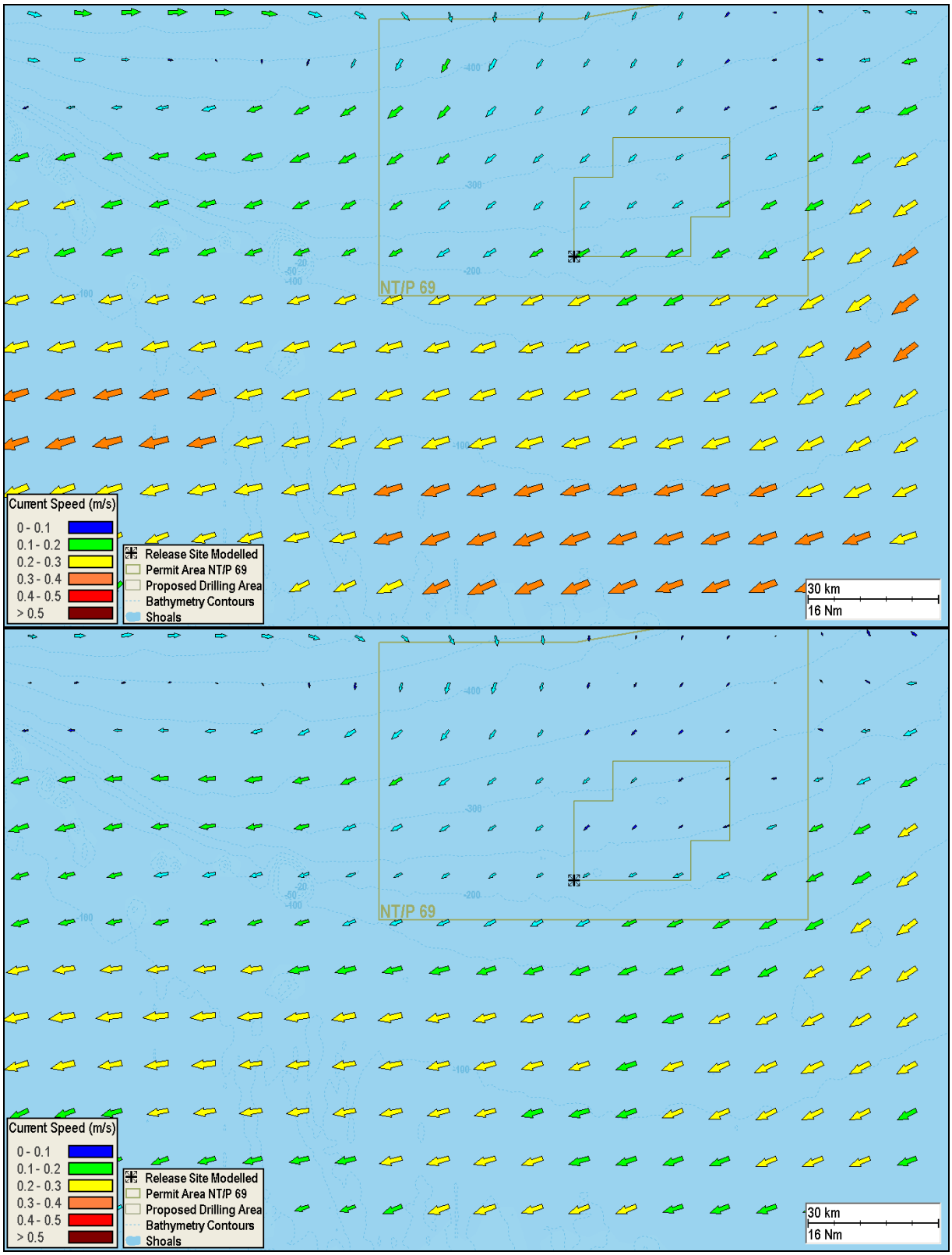

Figure 11: Screenshot of the surface (top image) and bottom (lower image) net (combined ocean and tidal) currents at 12 am 1st April 2004.

3 Water Temperature and Salinity Profile

The influence of temperature and salinity variations on sediment plumes in the far-field is negligible, these parameters were included as input into the model for completeness (see Table 3). Temperature and salinity data was obtained from the National Oceanographic Data Centre – World Ocean Atlas 2005 (http://www.nodc.noaa.gov/OC5/indprod.html).

Table 3: Temperature and salinity data as a function of water depth near the modelled release site.

Depth (m)	*Temperature (ºC)*	*Salinity (ppt)*
0	28.4	34.4
50	27.4	34.4
100	23.2	34.7
200	15.3	35.5
300	11.2	35.6

4 DISPERSION MODELLING METHODOLOGY

4.1 Sediment Dispersion Model Description - MUDMAP

MUDMAP is a highly advanced three-dimensional plume model used by industry and regulators to aid in assessing the potential environmental effects from operational discharges such as drill cuttings, drilling fluids and produced water. Since its inception in 1994, the model has been applied to hundreds of assessments in over 35 countries, including Australia (since 1996).

The model itself is an enhancement of the Offshore Operators Committee (OOC (Brandsma and Sauer, 1983)) model and calculates the fates of discharges through three distinct stages, as defined by laboratory and field studies (Koh and Chang, 1973; Khondaker, 1999):

Stage 1: **Convective decent** – free fall of the combined mass of fluids and cuttings;

Stage 2: **Dynamic collapse stage** – the collapse of the combined mass as it loses the initial jet related momentum and turbulence; and

Stage 3: **Dispersion stage** – model predicts the transport and dispersion of the discharged fluids and cuttings by the local currents. Dispersion of the discharged material will

be enhanced with increased current speeds and water depth and with greater variation in current direction over time and depth.

Each stage plays an integral role at different times and distance scales. The governing equations and solutions were built on the formulas originally developed by Koh and Chang (1973) and are extended by the work of Brandsma and Sauer (1983), known as the OOC model, for Stages 1 and 2 of plume motion.

The far-field calculation (passive dispersion stage), however, employs a particle-based, random walk procedure. The model predicts the dynamics of the discharge material and resulting seabed concentrations and bottom thicknesses over the near field (i.e. the immediate area of the discharge) and the far-field (the wider region). Figure 12 shows a conceptual diagram of the dispersion and fates of drill cuttings and fluids discharge to the ocean and the idealized representation of the three discharge phases.

Along with the advanced analyses tools, MUDMAP can simulate six classes (or 36 subcategories), each with its own density and particle size distribution. This means that the fluids, cuttings, water and chemicals can be included in the near-field and far-field computations. The discharged material is represented by a large sample of Lagrangian particles (32,000). During the dispersion stage, the particles are transported in three-dimensions according to the current data and horizontal and vertical mixing coefficients at each time step according to the governing equations.

MUDMAP has been extensively validated and applied for discharge operations in Australian coastal waters (e.g. Burns et. al., 1999; King and McAllister, 1997, 1998; Spaulding, 1994). A document titled “A review of models in support of oil and gas exploration off the North Coast of British Columbia”, prepared by the Institute of Ocean Sciences Fisheries and Oceans Canada (Foreman et al., 2005) stated that “for a drilling mud model, we feel that MUDMAP seems to be the best choice.”

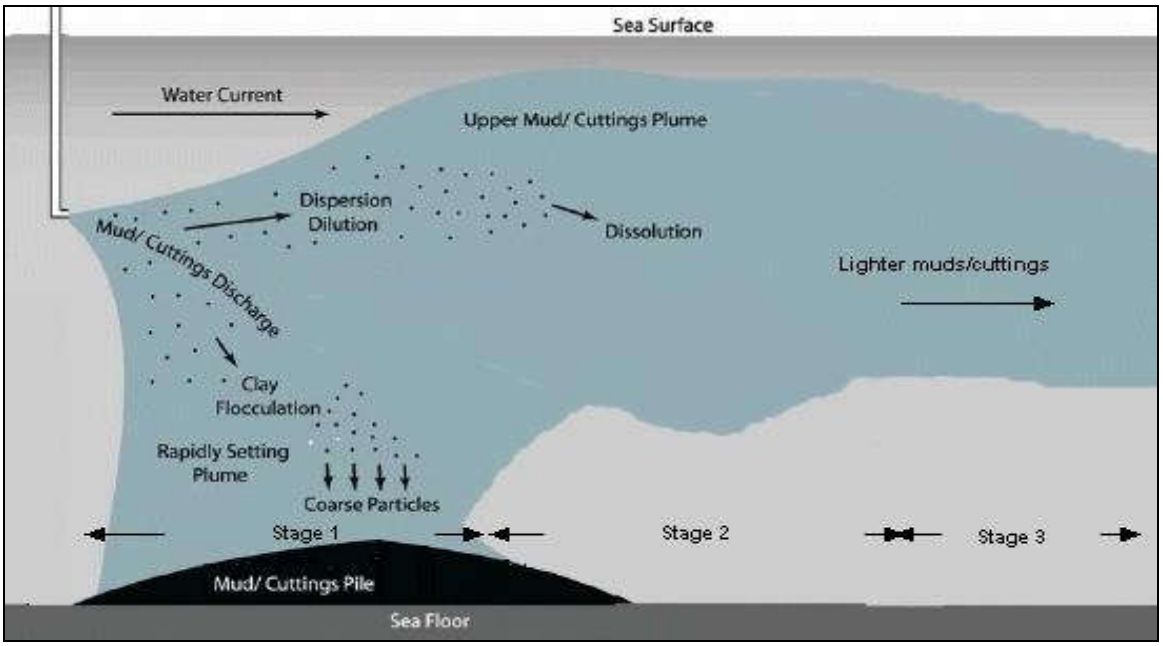

Figure 12: Conceptual diagram showing the general behaviour of cuttings and fluids (muds) following the discharge to the ocean (Neff, 2005) and the idealised representation of the three discharge phases.

4.2 Well Construction and Drilling Discharge

The first interval in the well will be the conductor section. A 36” conductor hole will be drilled riserless using seawater and high viscosity sweeps with all cuttings and drilling mud returned to the sea floor. The second interval in the well will be the surface section. A 17.5" surface hole will be drilled riserless using seawater and high viscosity sweeps. All drill fluids and drill cuttings will be returned to the seabed during the drilling of this section.

A 12.25" hole section will be drilled with synthetic based drilling fluid. Additionally, the 8.5" section will also be drilled using a synthetic based drilling fluid. The drill cuttings and fluids will be returned to the sea surface.

Approximately, 39.3 days of active drilling will be required to drill each well. Table 4 summarises the drilling fluid types and estimated volume of drill cuttings for each well interval.

Table 4: Drilling fluid types and estimated generated volumes of drill cuttings per well section.

Well interval	Hole diameter (inches)	Cuttings	Drilling fluid type		Point of discharge	Active drilling (days)
		Approximate volume (m^3) (Note 1)	Type	Approximate volume (m^3)		
Conductor hole	36	39	Seawater with high viscosity sweeps	100	*Seabed*	0.1
Surface hole	17.5	302	Seawater with high viscosity sweeps	1,542	*Seabed*	10.8
Intermediate hole	12.25	131	SBM	36*	*Sea surface**	9.9
Production hole	8.5	12	SBM	4*	*Sea surface**	18.5
	Total	**484**	**Total**	**1,642**	**Total**	**39.3**

Note 1: Volumes provided are best available estimates, calculated based on data acquitted from previous drilling activity undertaken by ConocoPhillips in the Bonaparte Basin.

** Best available estimates, calculated based on 10% oil on cuttings*

The input data into the dispersion model included:

- Volume and discharge duration of the cuttings and unrecoverable fluid solids;
- Sediment grain size distributions and associated settling velocities;
- Bulk density of the released material;
- Temperature and salinity profiles of the receiving waters;
- The size and orientation of the discharge pipe;
- The height of the point of discharge relative to mean sea level; and
- Current data to represent local physical forcing.

Table 5 shows a summary of the discharge configuration and model parameters used as input into the discharge model. All cuttings generated by riserless drilling of the 36” conductor hole and 17.5" surface hole will be returned to the seabed where they will accumulate in the vicinity of the wellhead. The drilling of conductor and surface hole sections typically takes approximately 10.9 days with the rate of discharge was assumed constant throughout the 10.9 day release. The model was run for a 15 day period to allow finer sediment to settle out of suspension.

The lower hole sections of each well, comprising the 12.25" and 8.5" sections, will be drilled using a recirculating drilling fluid system. Drilling time of the two lower sections is estimated at approximately 28.4 days, during which time the rate of discharge was assumed constant. The model was run for a total duration of 32 days to allow finer sediment to settle out of suspension. A marine riser run between the blowout preventer (BOP) and the mobile offshore drilling unit (MODU) will provide a conduit for the return of drilling fluid and cuttings back to the MODU. On the MODU the drilled cuttings and drilling fluid will be separated and cleaned using solids control equipment. After recovery of drill fluids, the drill cuttings will be discharged from the MODU at the well site to the sea surface.

The density of the cuttings and drilling fluids were assumed at 2,550 kg/m^3 and 4,200 kg/m^3, respectively (Nedweed, 2004). Based on the volumes of cuttings and fluids released, the bulk density for the seabed and sea surface discharges was approximately 3,916 kg/m^3 and 2,911 kg/m^3, respectively. It is important to note that grain size (in turn settling velocity) has a greater influence on the rate of settling than density (Neff, 2005).

Table 5: Input data used for the drill cuttings and muds dispersion modelling.

Parameter/description	*Detail*
Volume of cuttings discharged at the seabed	341 m^3
Volume of drilling fluid discharged at the seabed	1,642 m^3
Volume of cuttings discharged at the sea surface	143 m^3
Total volume of cuttings discharged	484 m^3
Total volume of drilling fluid discharged	1,642 m^3
Density of drill cuttings	2,550 kg/m^3
Density of drilling fluid	4,200 kg/m^3
Seabed discharge duration [model duration]	10.9 days [15 days]
Sea surface discharge duration [model duration]	28.4 days [32 days]
Depth of seabed discharge	2 m above seabed
Depth of sea surface discharge	Near the sea surface
Sea surface discharge pipe orientation	Vertically downward
Ocean current (see note 1)	- BLUElink ReANalysis model (BRAN) - Hourly dataset for 2004 - High resolution dataset spanning entire grid domain
Tidal currents (see note 1)	- Currents generated using ASA advanced ocean/coastal model (HYDROMAP) - Hourly dataset for 2004 - Validated currents against six observation tide stations
Water temperature and salinity (see note 2)	Regional specific seasonal sea surface temperature and salinity values

Note 1: CSIRO BLUElink ReANalysis deep ocean model and APASA Ocean/Coastal model, HYDROMAP

Note 2: National Oceanographic Data Centre, 2005 World Ocean Atlas

Table 6 shows the sediment grain sizes, settling velocities and distributions according to the fluid type and fluid to solids ratio for each well interval, as confirmed by the ConocoPhillips geoscience team.

The conductor and surface well intervals are to be drilled with seawater and high viscosity sweeps and the grain sizes are expected to range from 0.016 mm to 6 mm. The intermediate and production holes are to be drilled with synthetic based drilling fluid and the grain sizes are expected to range between 0.026 mm to 6 mm.

The settling velocity for each sediment grain size was obtained from empirical data provided by Dyer (1986). As can be seen in Table 6, settling velocities vary significantly between the smallest and largest grain sizes.

Table 6: Sediment grain size, settling velocities and distribution for each well interval according to fluid type and fluid to solids ratio.

Class	Sediment grain size (mm)	Settling velocity (cm/s)	Conductor and surface holes (%)	Intermediate and production holes (%)
Large cuttings	6	53.62	2.1	9.4
	5	49.46	2.1	9.4
	2	28.55	2.1	9.4
	1	12.73	1.4	6.3
	0.5	7.5	1.4	6.3
	0.45	6.6	0.7	3.1
Medium cuttings	0.4	6	0.7	3.1
	0.35	5	0.7	3.1
	0.3	4	0.7	3.1
	0.25	3.1	0.7	3.1
	0.2	2.3	0.7	3.1
	0.15	1.6	0.7	3.1
Small cuttings	0.1	0.8	0.7	3.1
	0.05	0.22	0.7	3.1
	0.04	0.15	0.7	3.1
	0.03	0.08	0.7	6.2
	0.02	0.04	0.7	0.0
Drilling fluid solids	0.063	0.34	1.2	0.0
	0.05	0.22	4.5	1.2
	0.035	0.11	10.7	2.9
	0.026	0.06	17.4	17.8
	0.02	0.038	21.6	0.0
	0.016	0.026	27.4	0.0

4.3 Grid Configuration

To calculate the concentrations from the seabed discharges, each horizontal grid cell size was 20 m x 20 m, covering a 20 km (longitude, x-direction) x 20 km (latitude, y-direction) extent around the release location. For the sea surface discharges, each horizontal grid cell was 10 m x 10 m grid covering a 10 km x 10 km extent around the release location.

4.4 Bathymetry

A combination of datasets was used to describe the shape of the sea bed and resolve the nearby shoals. Data from Geoscience Australia national bathymetric dataset, which has a nominal resolution of approximately 250 m, were interpolated spatially with spot and contour depths from recent electronic nautical charts to form a seamless, highly accurate representation of the seabed (Geoscience Australia, 2009).

4.5 Mixing Parameters

For discharges at the sea surface, a horizontal coefficient value of 0.25 m^2/s was used as model input to account for the turbulence of the sediment as it is transported from the release site. A vertical coefficient value of 0.1 m^2/s was used as model input to account for the influence of turbulence within the water column, as well as wave induced turbulence. Values are based on previous studies by Copeland (1996).

For the discharge of cuttings and drilling fluids near the seabed, the horizontal dispersion coefficient used was 0.25 m^2/s; however, a very low vertical parameter was set (0.0001 m^2/sec), as vertical turbulence is negligible at 2 m above the seabed.

5 RESULTS

5.1 Presentation of Model Results

The predicted total sediment deposition from the near seabed and surface discharges from the release site are presented in Sections 5.2 and 5.3, respectively.

As the MUDMAP model is able to track sediment to thicknesses that are lower than biologically significant levels, it was necessary to specify a minimum threshold for the results which would record the "coverage" on the seafloor above the natural sedimentation.

The natural sedimentation threshold was determined from a digital database compiled by the National Geophysical Data Center (NGDC) within the United States. The database indicates that the annual natural sedimentation rate for the study region is approximately 60 g/m^2, which is typical of Australian ocean environments. This equated to an approximate minimum threshold of 10 g/m^2 total (non-temporal, total load) over the entire modelling period and a conservative thickness of 0.0026 mm.

To aid in the interpretation of model results, bottom deposition is presented as both mass per area (g/m^2) as well as thickness (mm).

5.2 Seabed Discharges

No contact was predicted (above a bottom deposition threshold of 10 g/m^2) for Evans Shoal and Tassie Shoal from the seabed discharges at the release location for any of the 12 modelling commencement months. The predicted minimum distance from Evans Shoal and Tassie Shoal to the 10 g/m^2 contour was 53.1 km and 62.0 km, respectively.

Figure 13 to Figure 24 show the predicted area covered (greater than 10 g/m^2) from discharges at the seabed, under varying current conditions for the start of each calendar month (January to December).

Table 7 shows the predicted maximum seabed deposition and area of coverage (above 10 g/m^2) for each seabed discharge simulation. The highest predicted sediment thickness (between 361 mm to 432 mm) was predicted to occur immediately adjacent to the release site within a 20 m x 20 m area. Within 100 m from the release site, the average and maximum bottom thickness decreased to 4.5 mm and 11 mm, respectively.

The modelling results showed that due to the height of the model release (modelled at 2 m above the seabed) the currents had little influence on the larger sediment (>150 mm diameter) which readily settled within 60 m south from the release site. The currents did have an effect on the transport of the smaller sediment (<0.15 mm diameter), which were predicted to will be carried further away from the release site (up to 3-4 km), due to slower settling velocities, in varying directions as a very thin layer of sediments.

Table 7: Summary of the maximum predicted bottom thicknesses and area of coverage for the seabed discharge simulations, initiated on the first day of each month. Also shown is the minimum distance from sensitive receptors to the 10 g/m^2 contour.

Commencement month	***Maximum bottom deposition (mm)***	***Total area of coverage above the natural sedimentation threshold of 10 g/m^2 or 0.0026 mm (km^2)***	***Minimum distance from the sensitive receptor to the 10 g/m^2 contour (km)***	
			Evans Shoal	***Tassie Shoal***
January	398	1.45	60.6	68.1
February	361	10.78	61.2	68.7
March	428	3.99	58.5	66.4
April	390	12.05	53.1	62.0
May	376	13.52	59.8	67.8
June	399	11.29	53.2	62.1
July	391	18.82	55.6	65.4
August	427	6.66	56.8	65.4
September	375	14.59	59.0	67.3
October	415	12.99	54.9	65.2
November	432	6.14	58.0	66.0
December	395	10.43	58.5	67.5
Minimum	**361**	**1.45**	**53.1**	**62.0**
Maximum	**432**	**18.82**	**61.2**	**68.7**

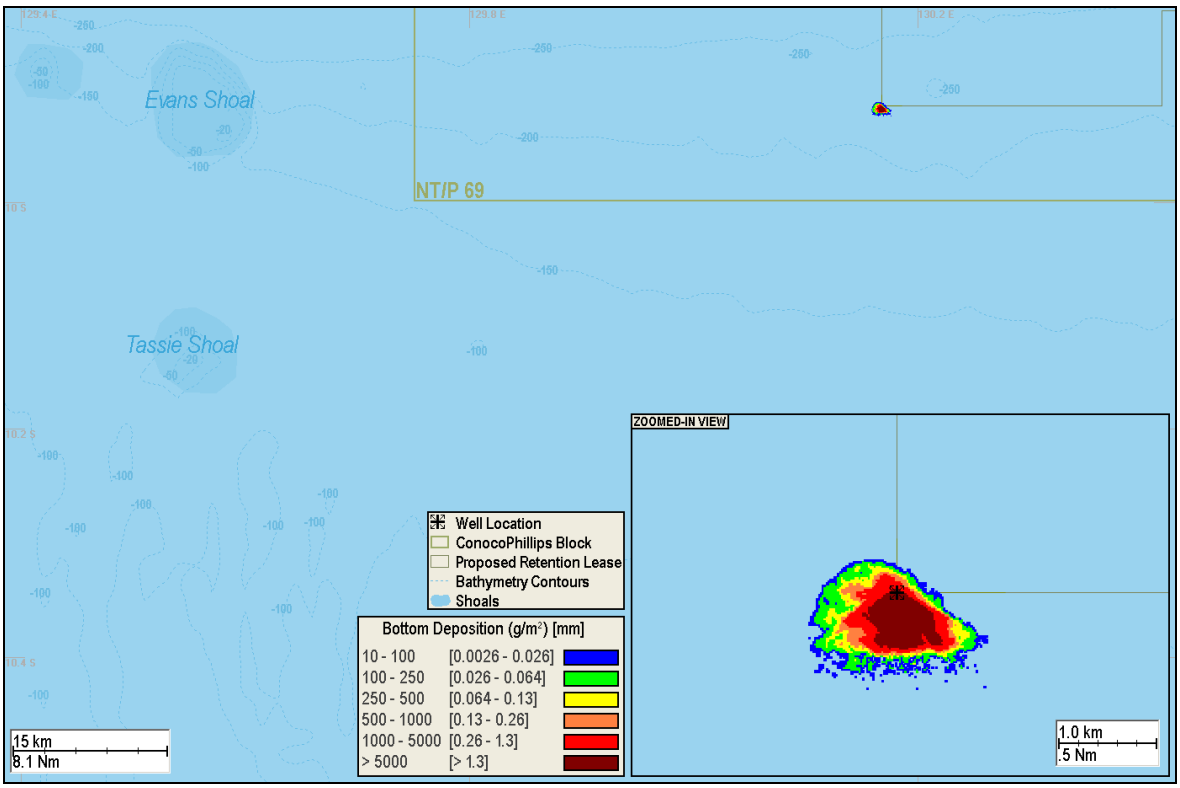

Figure 13: Predicted bottom deposition and seafloor coverage from the discharge of drill cuttings and fluids at the seabed, commencing in January. The inset shows a zoomed in view.

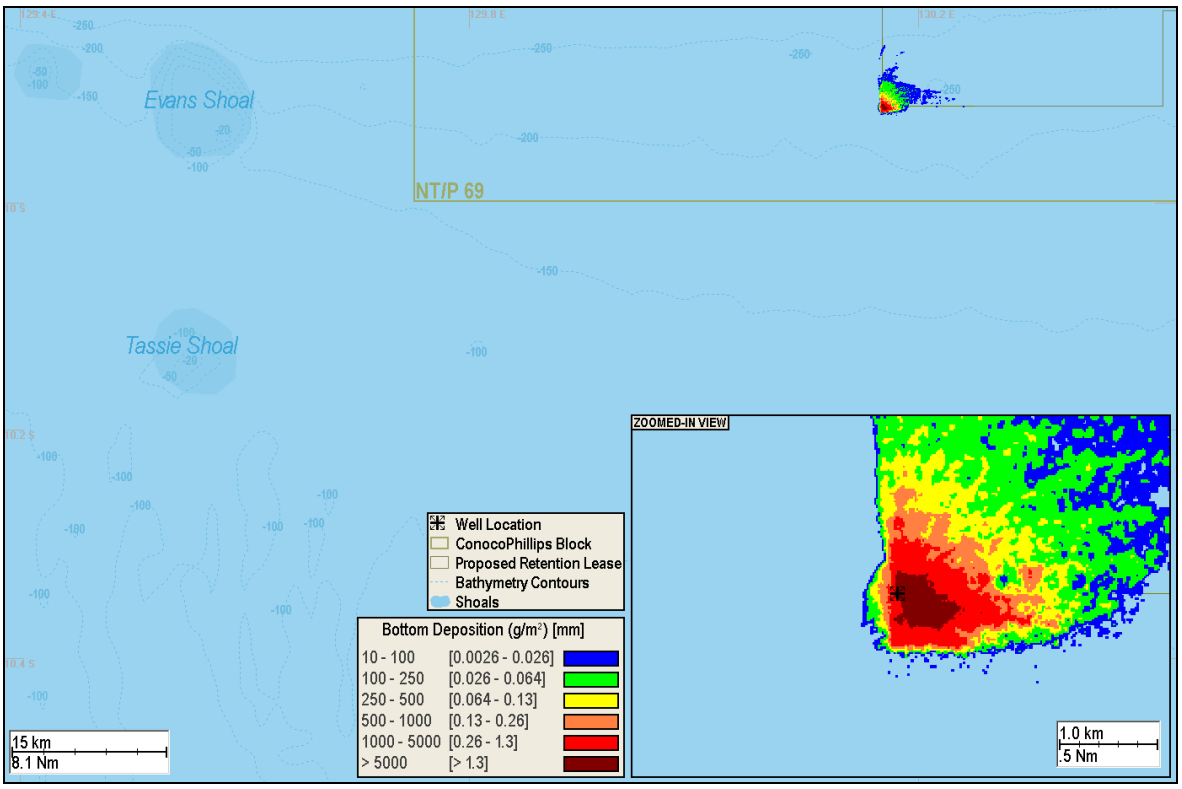

Figure 14: Predicted bottom deposition and seafloor coverage from the discharge of drill cuttings and fluids at the seabed, commencing in February. The inset shows a zoomed in view.

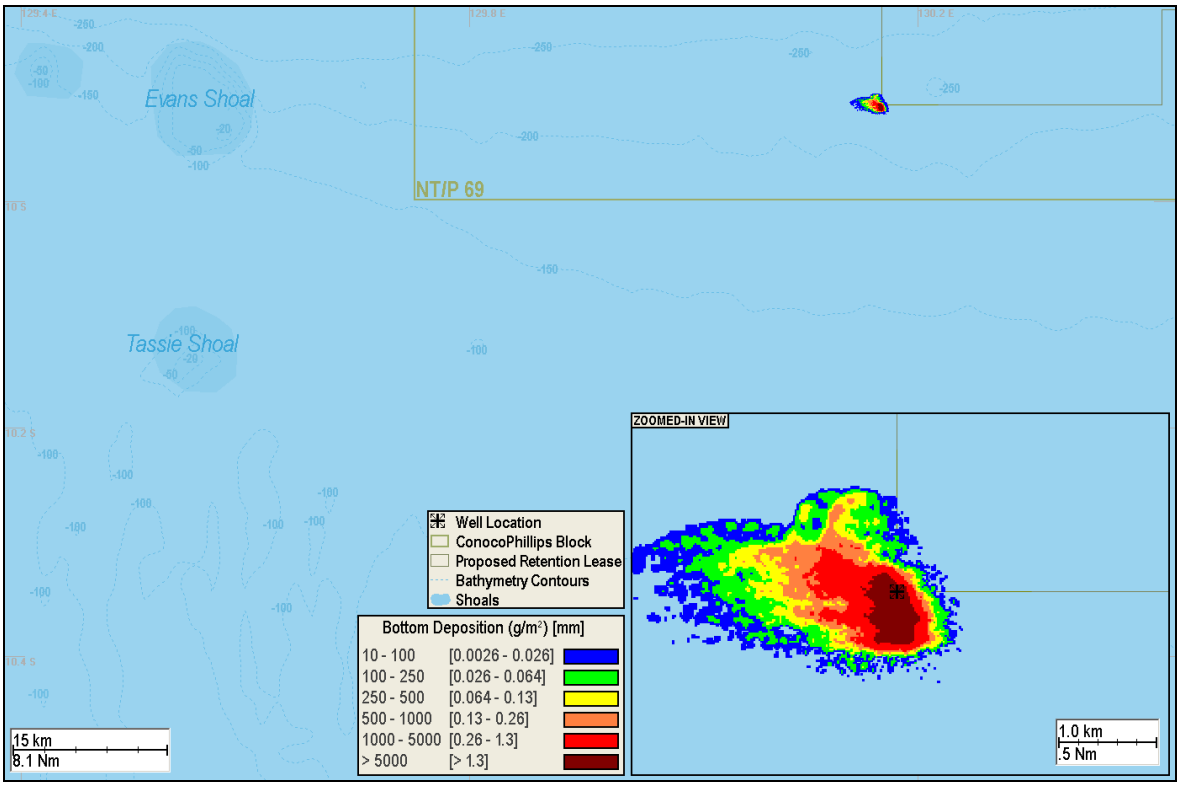

Figure 15: Predicted bottom deposition and seafloor coverage from the discharge of drill cuttings and fluids at the seabed, commencing in March. The inset shows a zoomed in view.

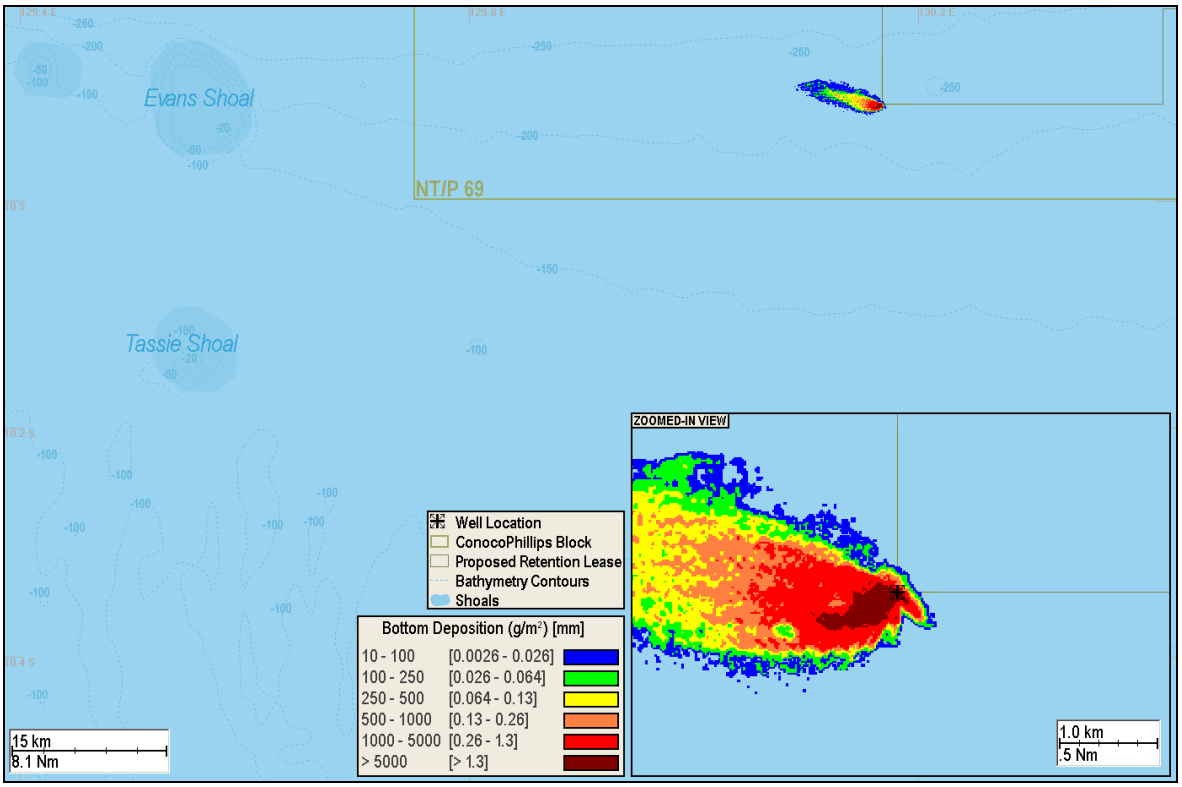

Figure 16: Predicted bottom deposition and seafloor coverage from the discharge of drill cuttings and fluids at the seabed, commencing in April. The inset shows a zoomed in view.

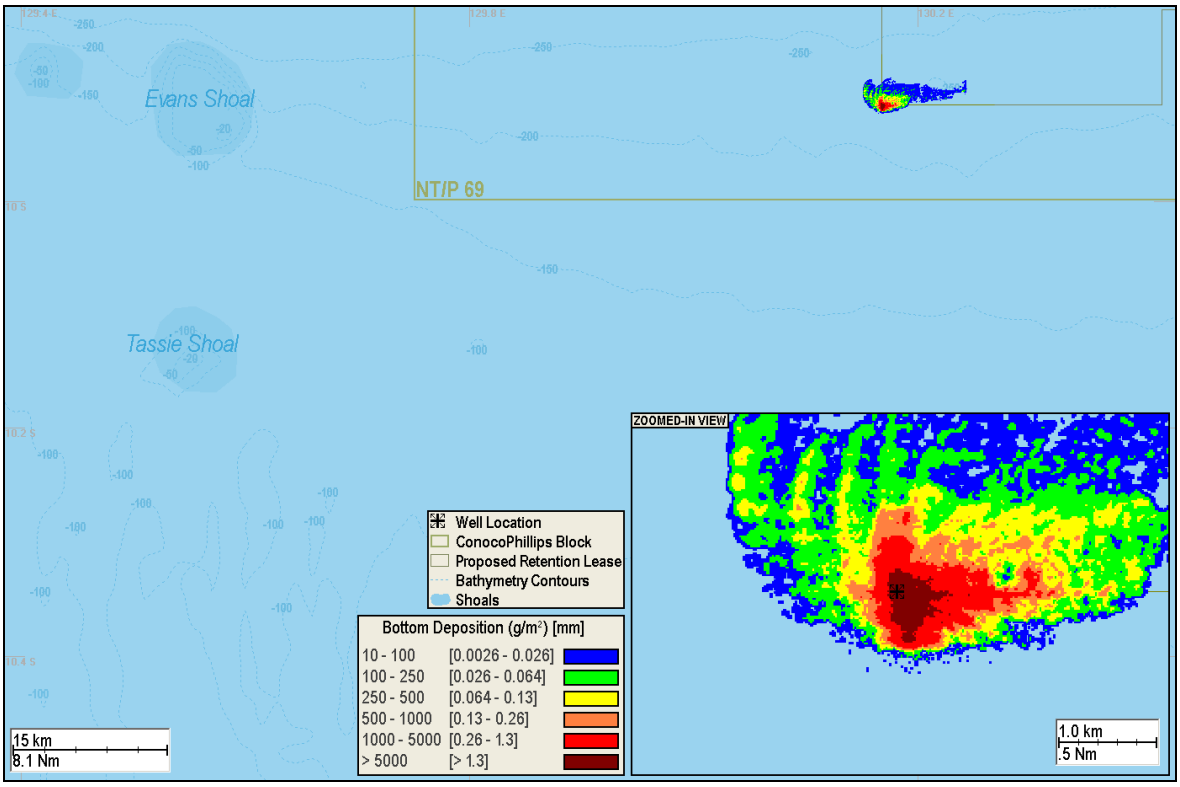

Figure 17: Predicted bottom deposition and seafloor coverage from the discharge of drill cuttings and fluids at the seabed, commencing in May. The inset shows a zoomed in view.

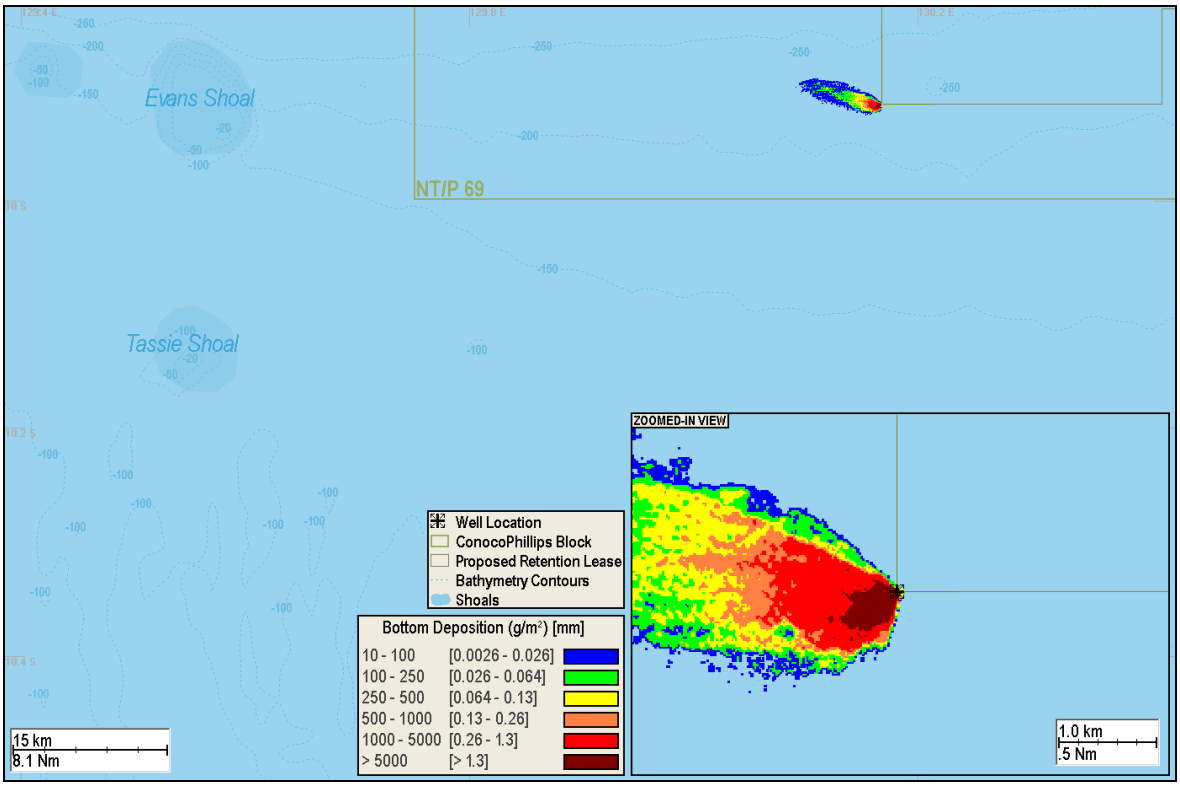

Figure 18: Predicted bottom deposition and seafloor coverage from the discharge of drill cuttings and fluids at the seabed, commencing in June. The inset shows a zoomed in view.

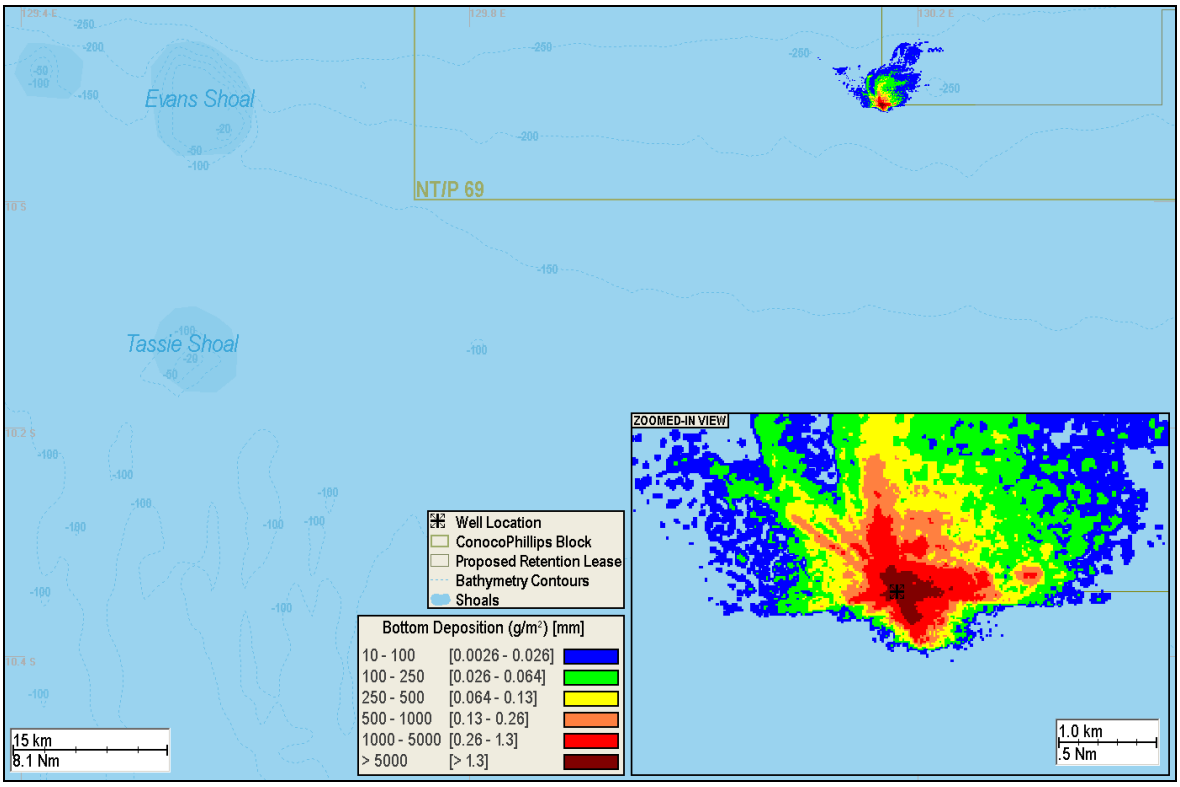

Figure 19: Predicted bottom deposition and seafloor coverage from the discharge of drill cuttings and fluids at the seabed, commencing in July. The inset shows a zoomed in view.

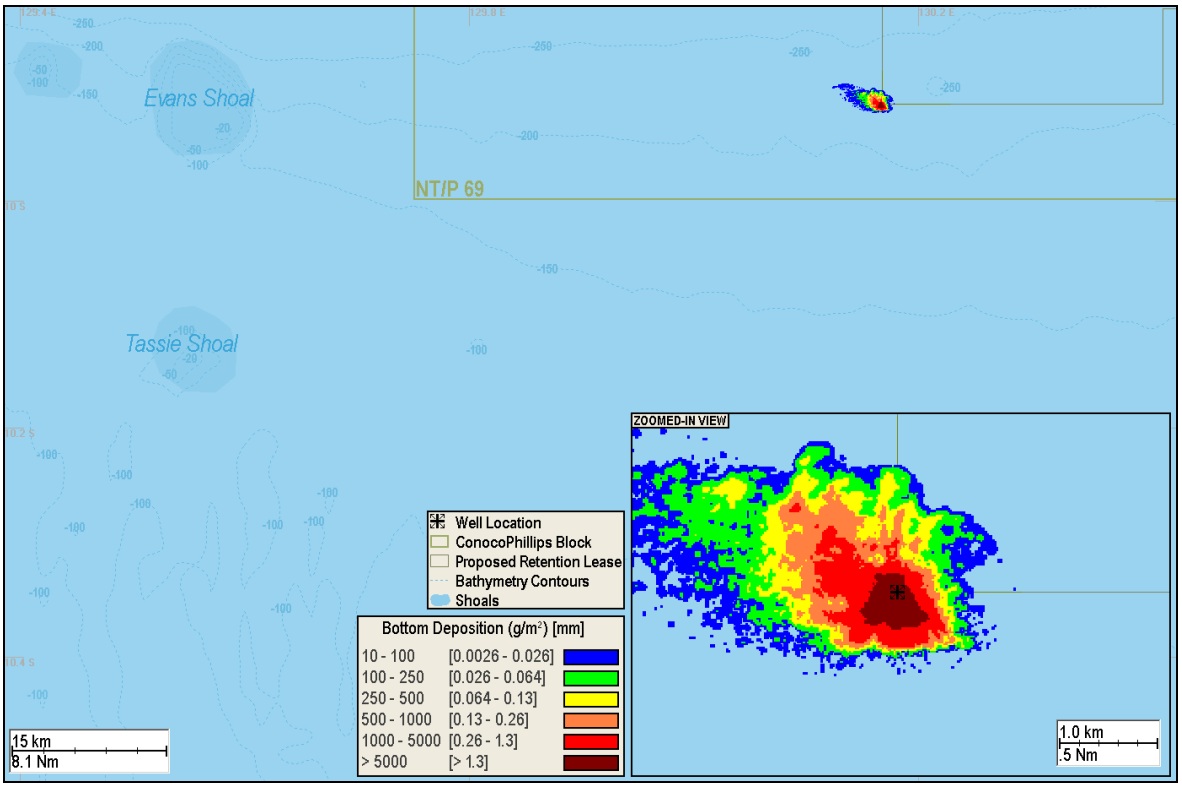

Figure 20: Predicted bottom deposition and seafloor coverage from the discharge of drill cuttings and fluids at the seabed, commencing in August. The inset shows a zoomed in view.

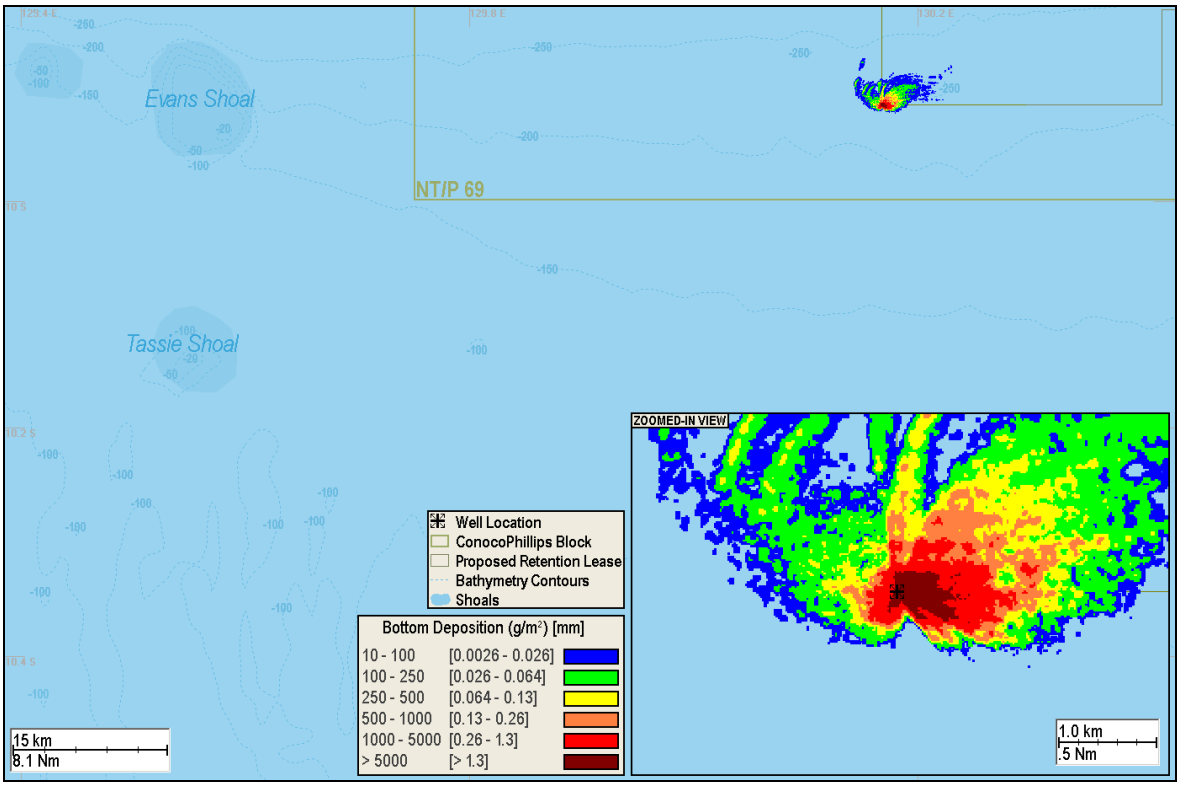

Figure 21: Predicted bottom deposition and seafloor coverage from the discharge of drill cuttings and fluids at the seabed, commencing in September. The inset shows a zoomed in view.

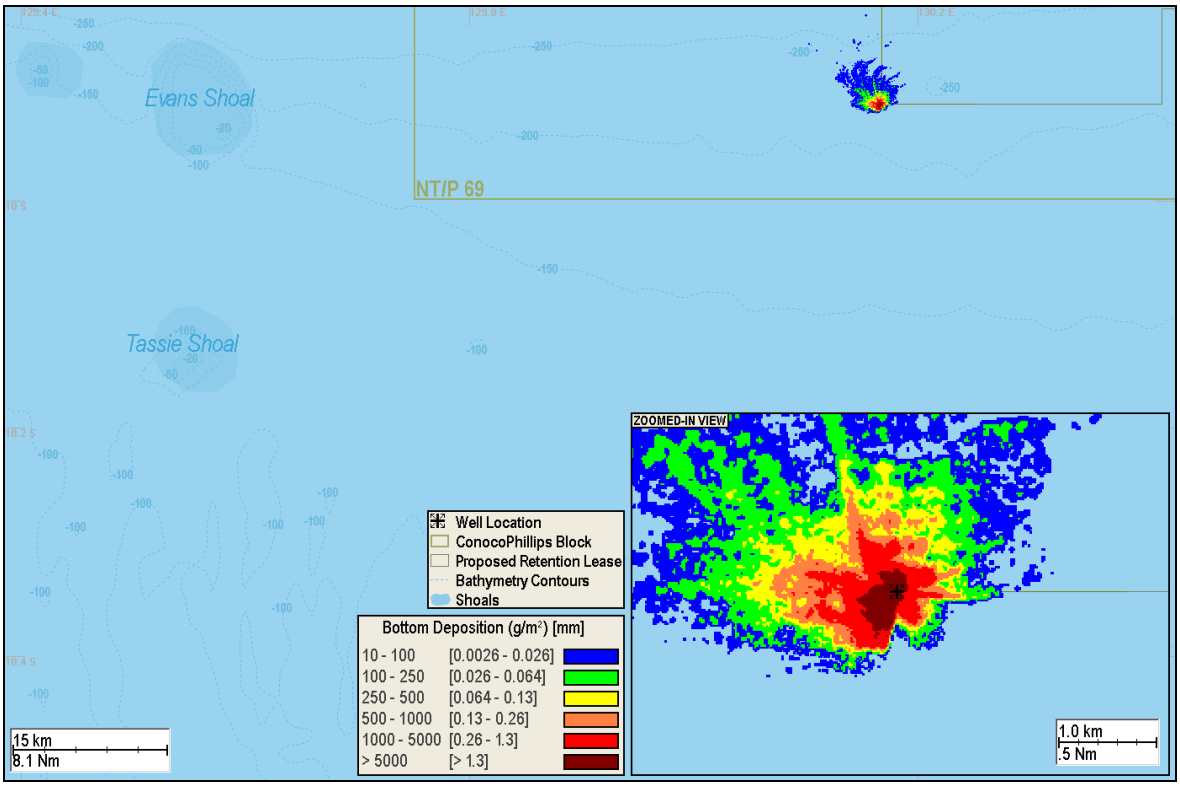

Figure 22: Predicted bottom deposition and seafloor coverage from the discharge of drill cuttings and fluids at the seabed, commencing in October. The inset shows a zoomed in view.

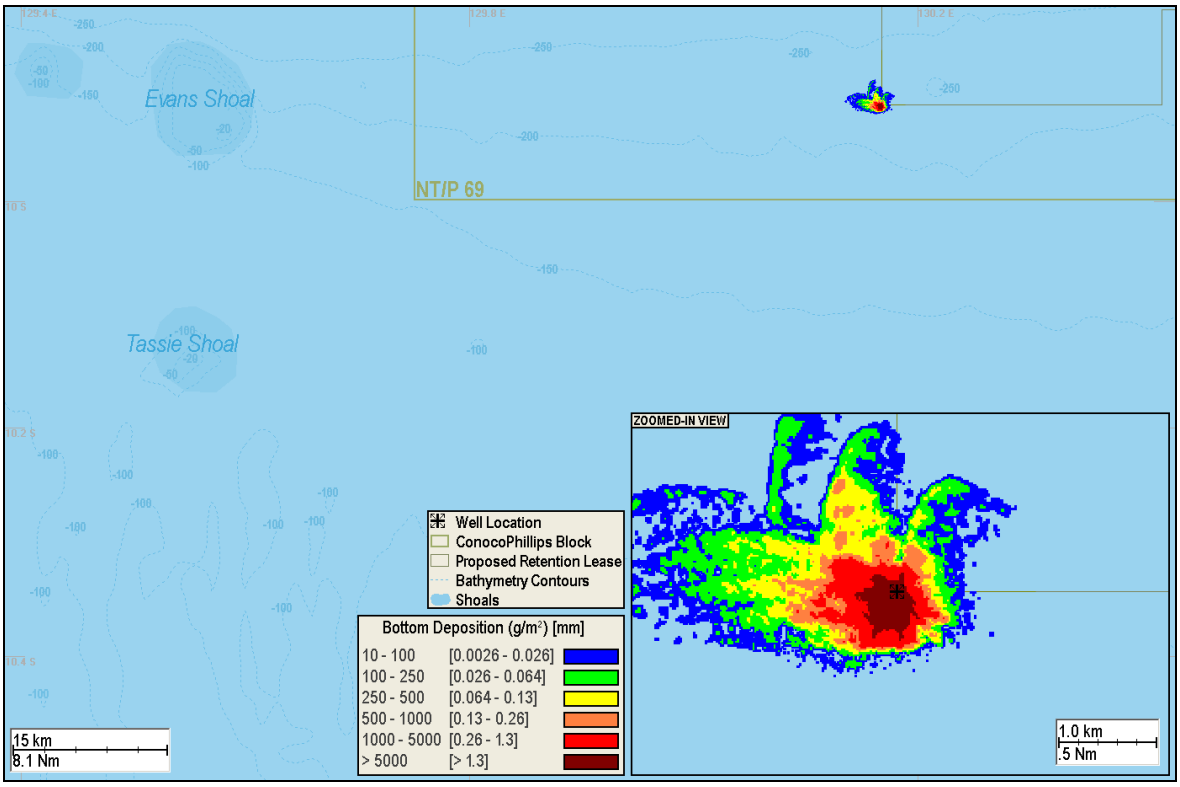

Figure 23: Predicted bottom deposition and seafloor coverage from the discharge of drill cuttings and fluids at the seabed, commencing in November. The inset shows a zoomed in view.

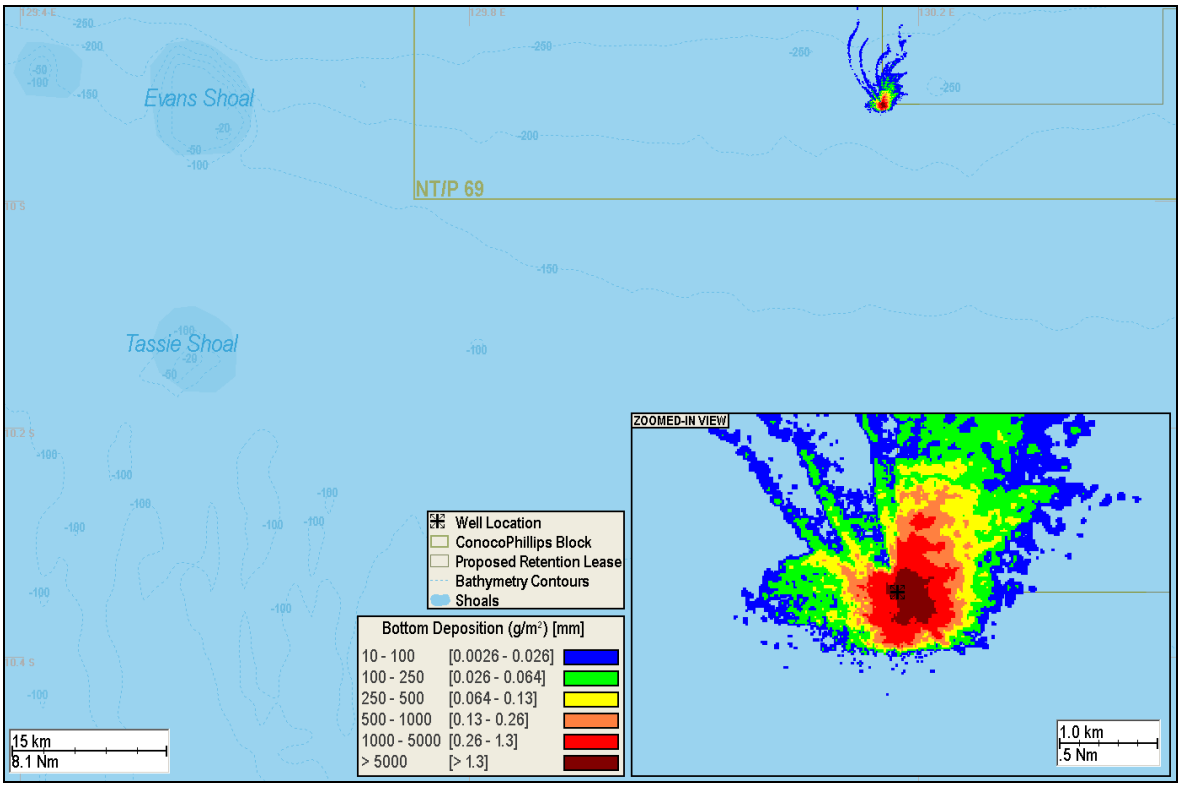

Figure 24: Predicted bottom deposition and seafloor coverage from the discharge of drill cuttings and fluids at the seabed, commencing in December. The inset shows a zoomed in view.

5.3 Sea Surface Discharges

No contact was predicted (above a bottom deposition threshold of 10 g/m^2) for Evans Shoal and Tassie Shoal from the sea surface discharges at the release location for any of the 12 modelling commencement months. The predicted minimum distance from Evans Shoal and Tassie Shoal to the 10 g/m^2 contour was 60.2 km and 67.9 km, respectively.

Figure 25 to Figure 36 show the predicted area covered (greater than 10 g/m^2) from discharges at the sea surface, under varying current conditions for the start of each calendar month (January to December).

Table 8 shows the predicted maximum seabed deposition and area of coverage (above 10 g/m^2) for each seabed discharge simulation. The seabed accumulation resulting from the sea surface discharges was much less compared to the seabed discharges and ranged from a maximum of 2 to 7 mm. Within 100 m from the release site, the predicted average and maximum bottom thickness was 0.5 mm and 2.4 mm, respectively. The modelling showed that with the sea surface releases occuring approximately 220 m above the seabed, the sediment was exposed to the force of the current for a longer period of time. Thus, transporting the material further away from the release site and causing it to settle over a larger area as a thinner pile.

Table 8: Summary of the maximum predicted bottom thicknesses and area of coverage for the sea surface discharge simulations, initiated on the first day of each month. Also shown is the minimum distance from sensitive receptors to the 10 g/m^2 contour.

Commencement month	***Maximum bottom deposition (mm)***	***Total area of coverage above the natural sedimentation threshold of 10 g/m^2 or 0.0034 mm (km^2)***	***Minimum distance from the sensitive receptor to the 10 g/m^2 contour (km)***	
			Evans Shoal	***Tassie Shoal***
January	6	1.11	61.0	68.6
February	2	0.78	60.2	67.9
March	3	1.23	60.5	68.3
April	6	1.05	60.7	68.4
May	4	1.27	60.5	68.2
June	2	0.63	60.9	68.6
July	3	1.21	60.5	68.3
August	5	1.10	61.0	68.7
September	6	0.99	60.5	68.3
October	4	1.20	60.5	68.3
November	7	1.04	60.8	68.5
December	5	1.18	60.7	68.4
Minimum	**2**	**0.63**	**60.2**	**67.9**
Maximum	**7**	**1.27**	**61.0**	**68.7**

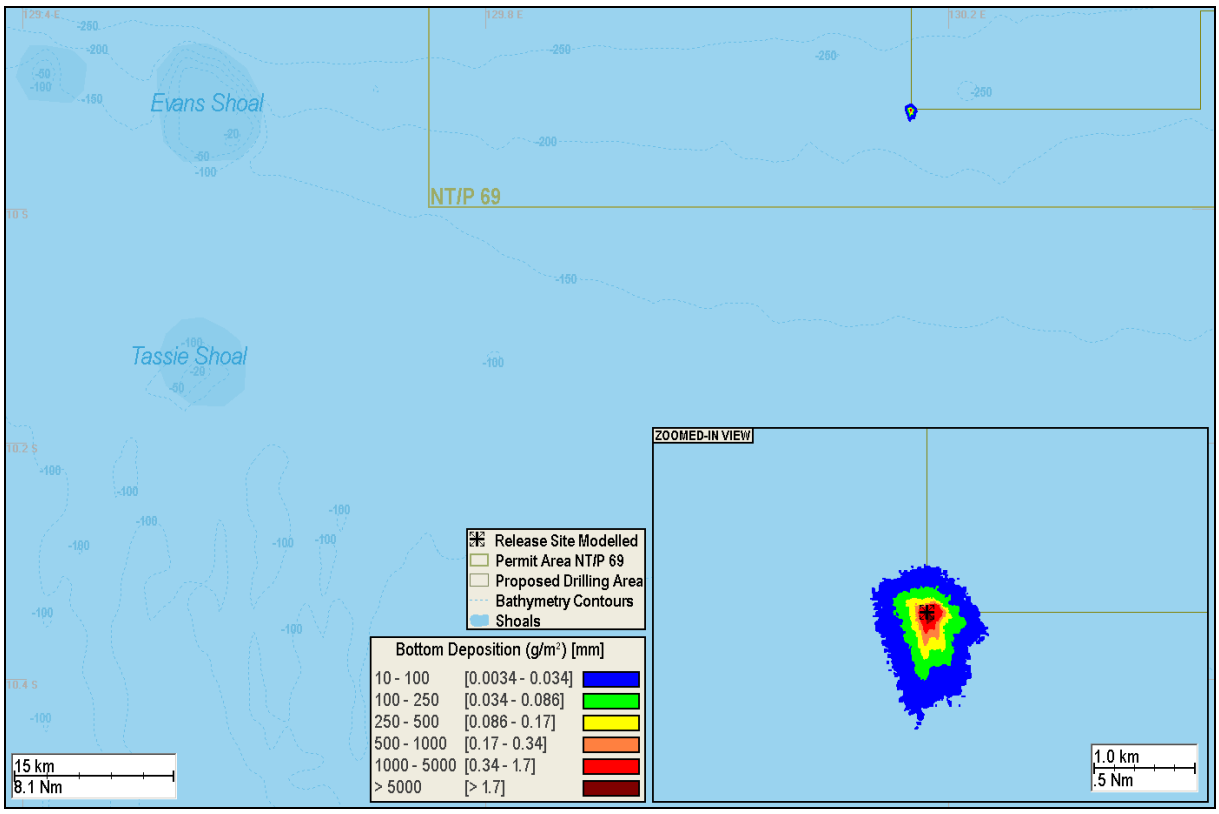

Figure 25: Predicted bottom deposition and seafloor coverage from the discharge of drill cuttings at the sea surface, commencing in January. The inset shows a zoomed in view.

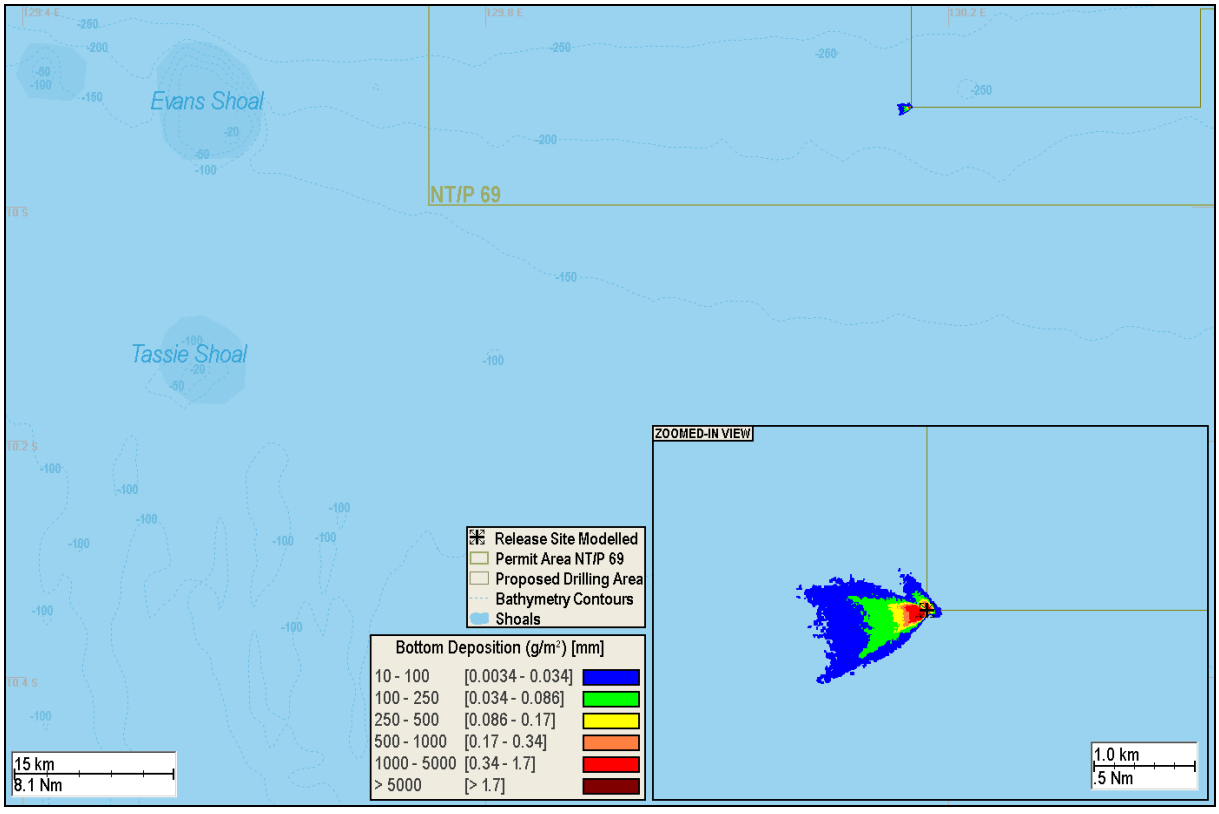

Figure 26: Predicted bottom deposition and seafloor coverage due to a 28.4 day discharge of drill cuttings at the sea surface, commencing in February. The inset shows a zoomed in view.

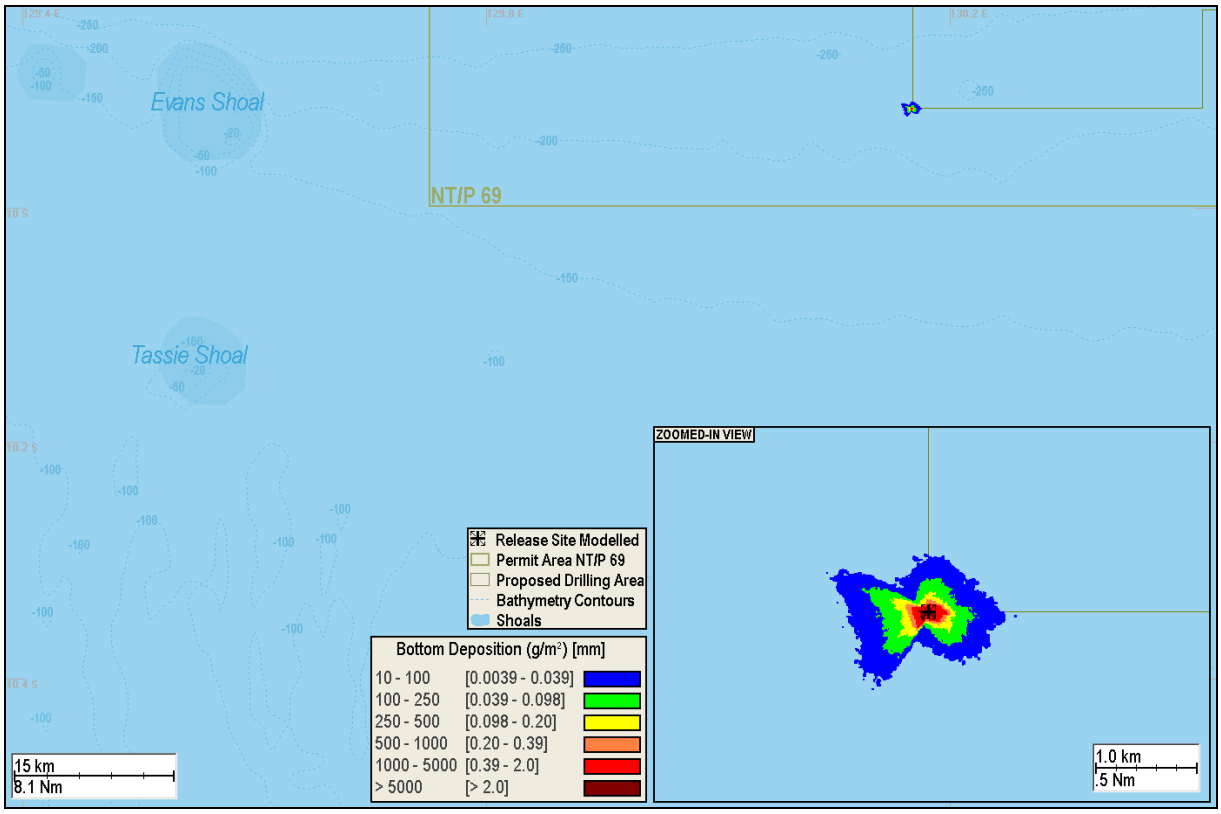

Figure 27: Predicted bottom deposition and seafloor coverage from the discharge of drill cuttings at the sea surface, commencing in March. The inset shows a zoomed in view.

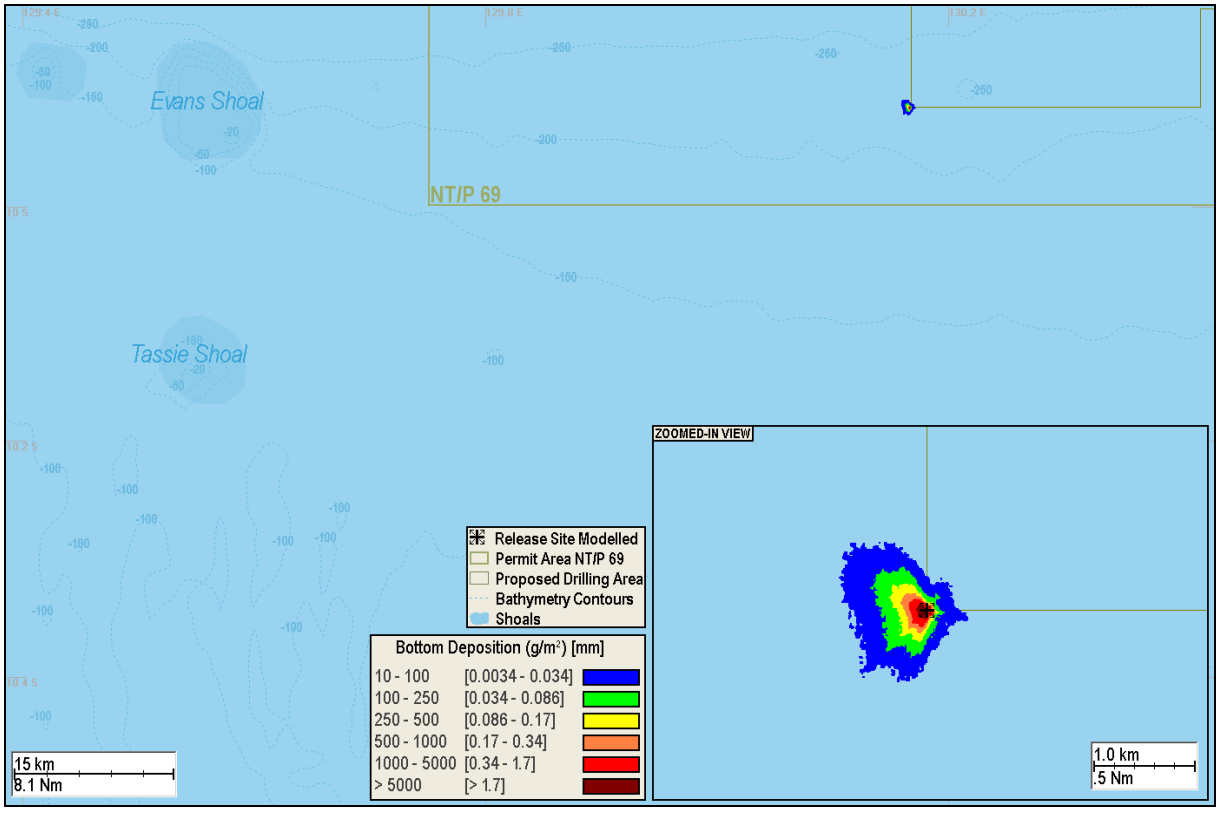

Figure 28: Predicted bottom deposition and seafloor coverage from the discharge of drill cuttings at the sea surface, commencing in April. The inset shows a zoomed in view.

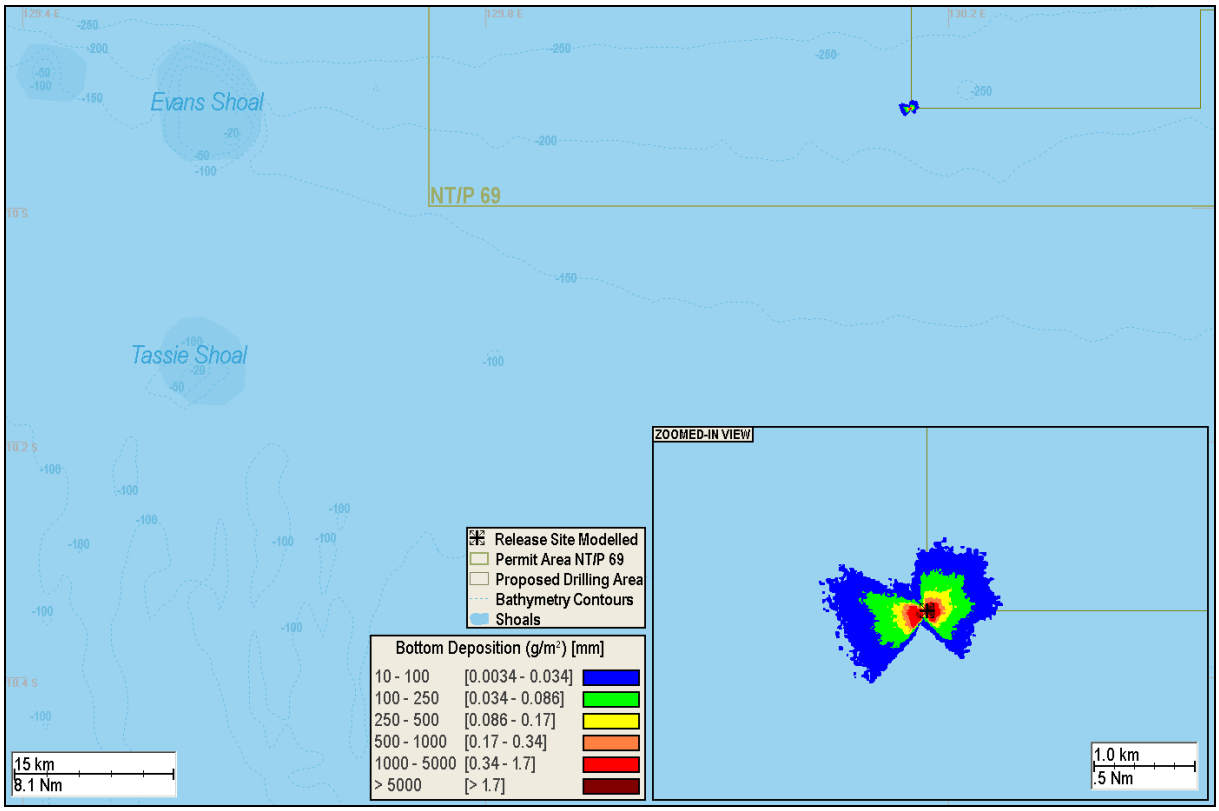

Figure 29: Predicted bottom deposition and seafloor coverage from the discharge of drill cuttings at the sea surface, commencing in May. The inset shows a zoomed in view.

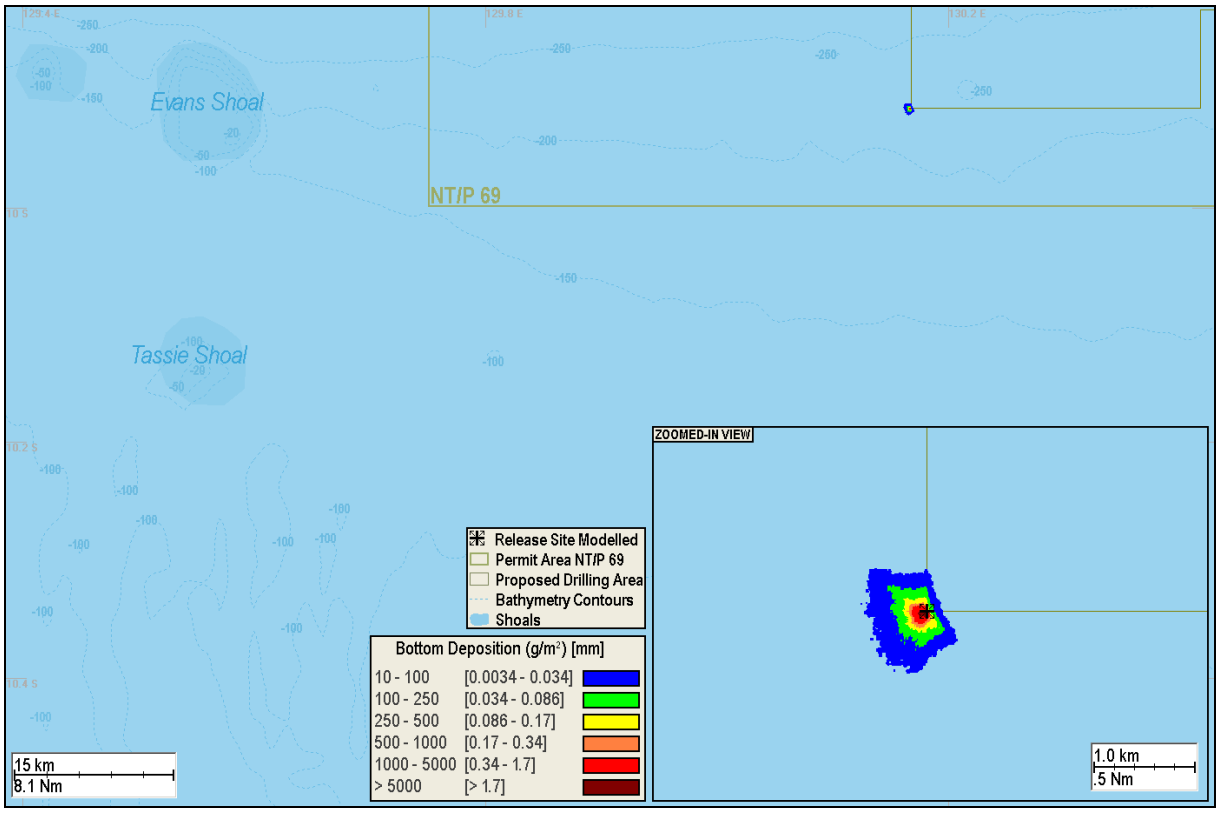

Figure 30: Predicted bottom deposition and seafloor coverage from the discharge of drill cuttings at the sea surface, commencing in June. The inset shows a zoomed in view.

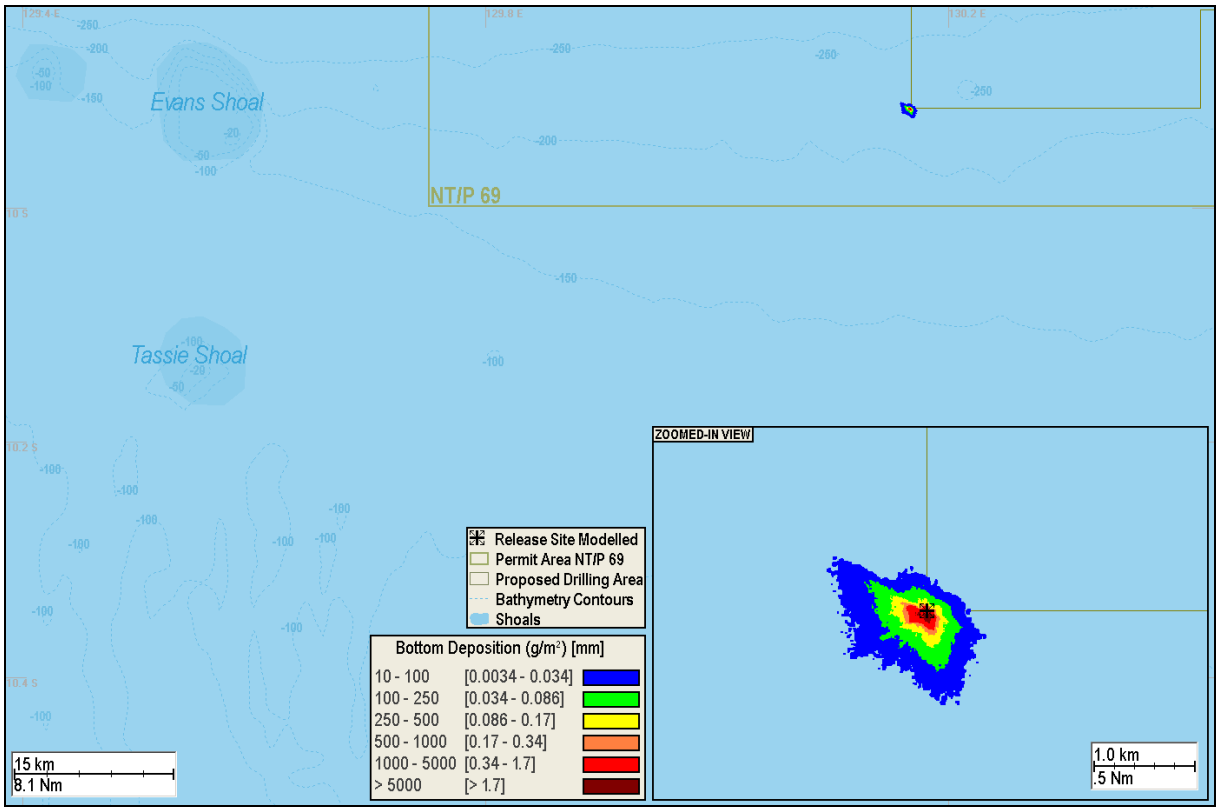

Figure 31: Predicted bottom deposition and seafloor coverage from the discharge of drill cuttings at the sea surface, commencing in July. The inset shows a zoomed in view.

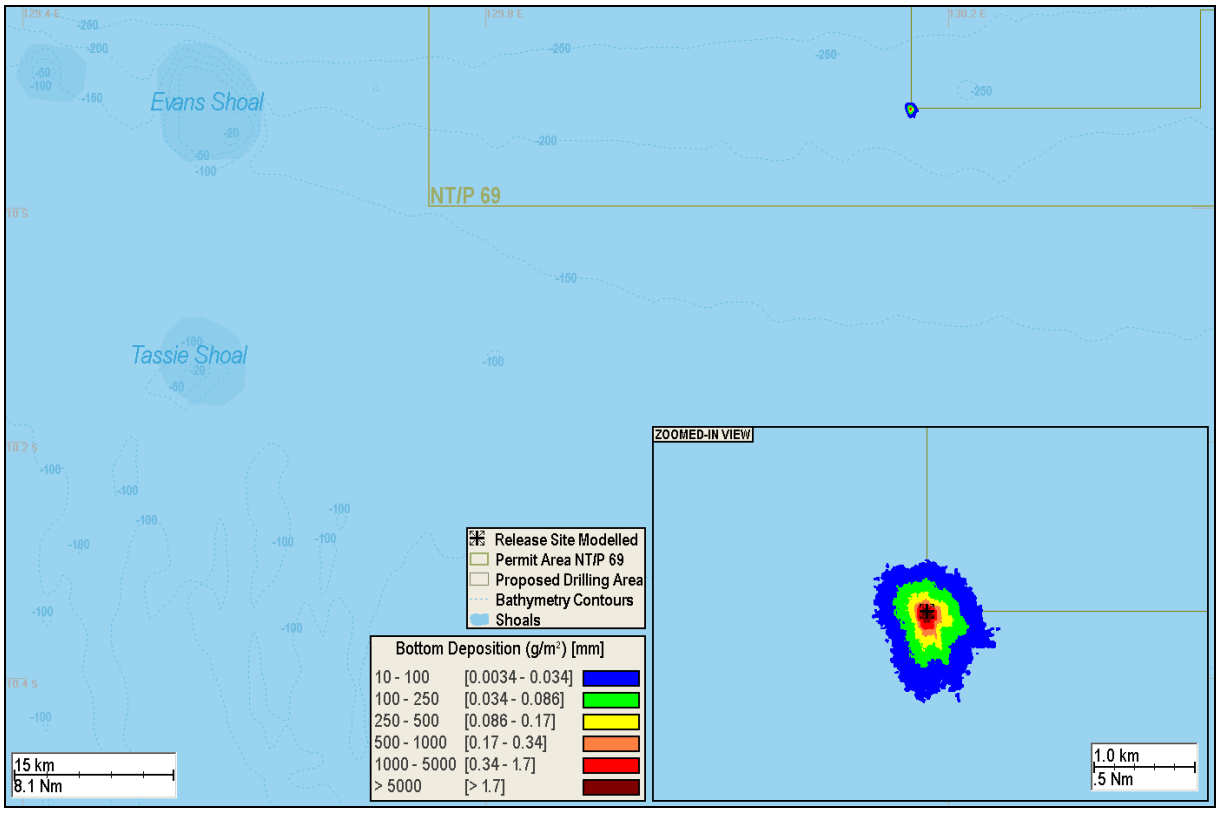

Figure 32: Predicted bottom deposition and seafloor coverage from the discharge of drill cuttings at the sea surface, commencing in August. The inset shows a zoomed in view.

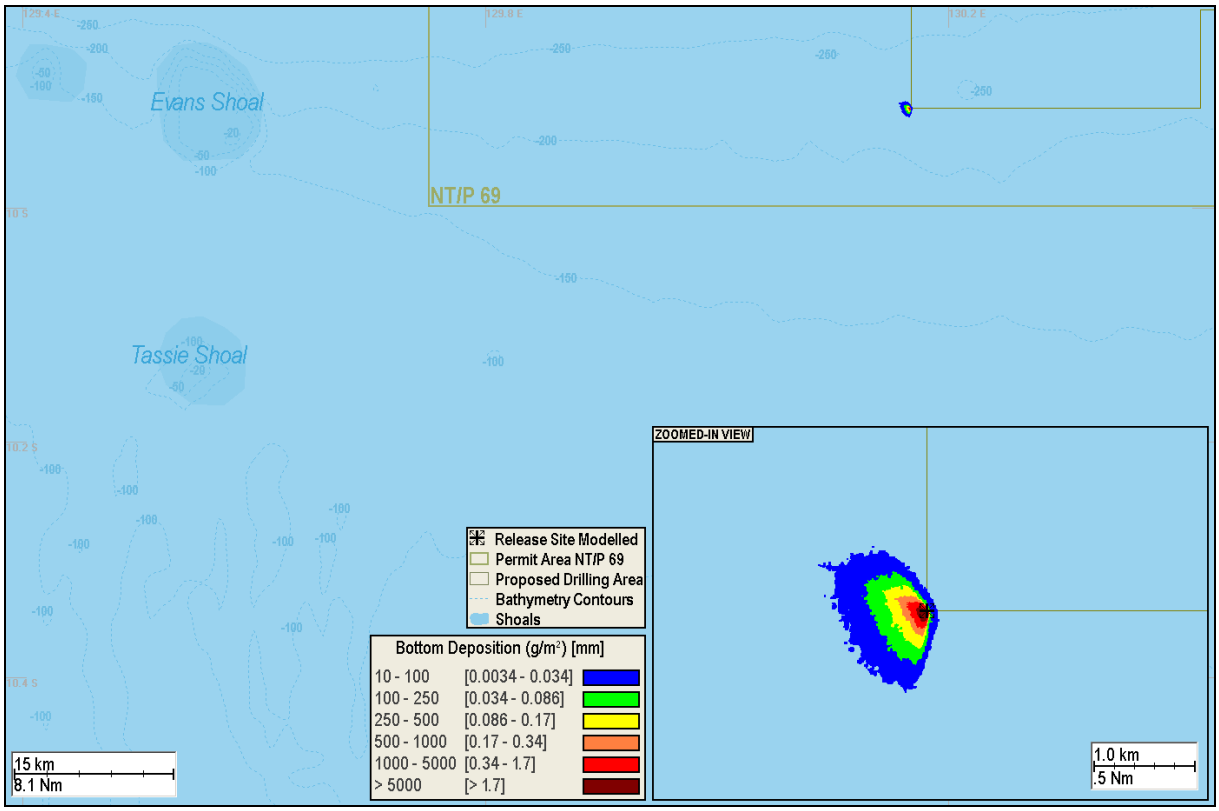

Figure 33: Predicted bottom deposition and seafloor coverage from the discharge of drill cuttings at the sea surface, commencing in September. The inset shows a zoomed in view.

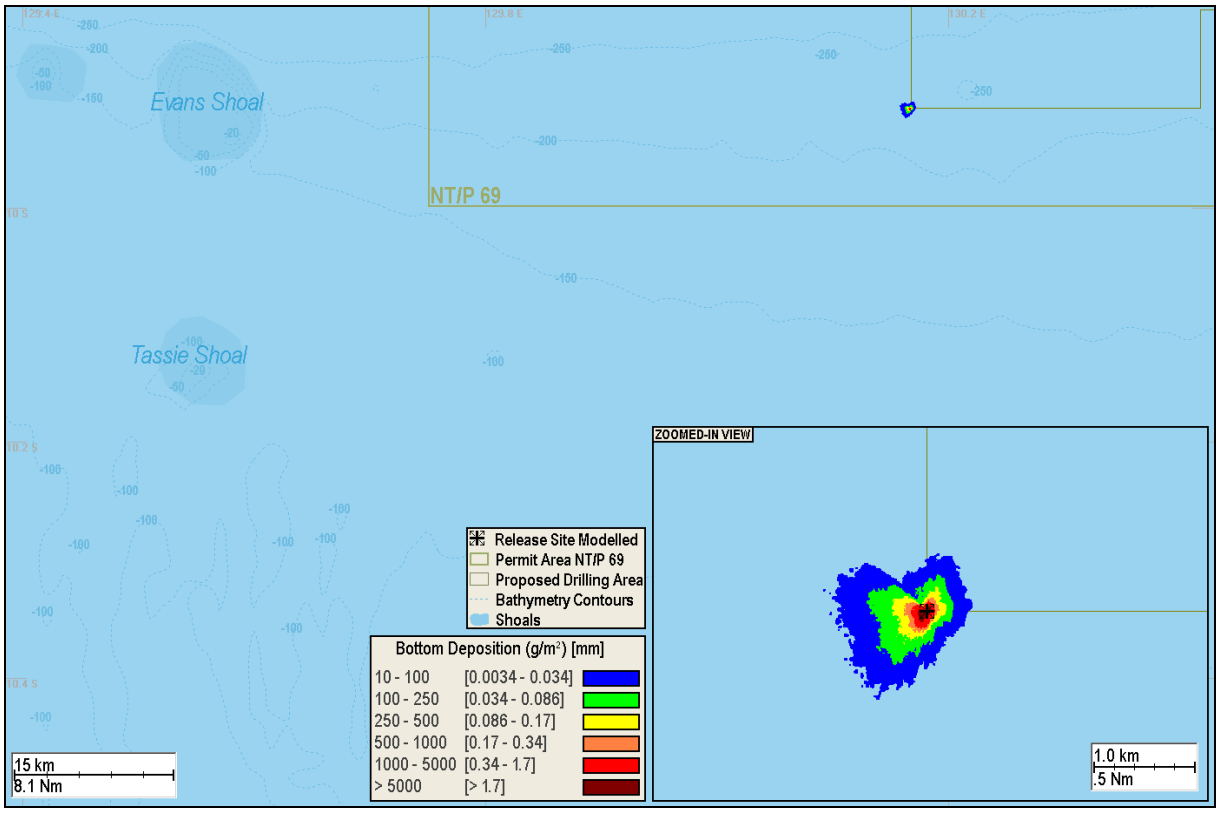

Figure 34: Predicted bottom deposition and seafloor coverage from the discharge of drill cuttings at the sea surface, commencing in October. The inset shows a zoomed in view.

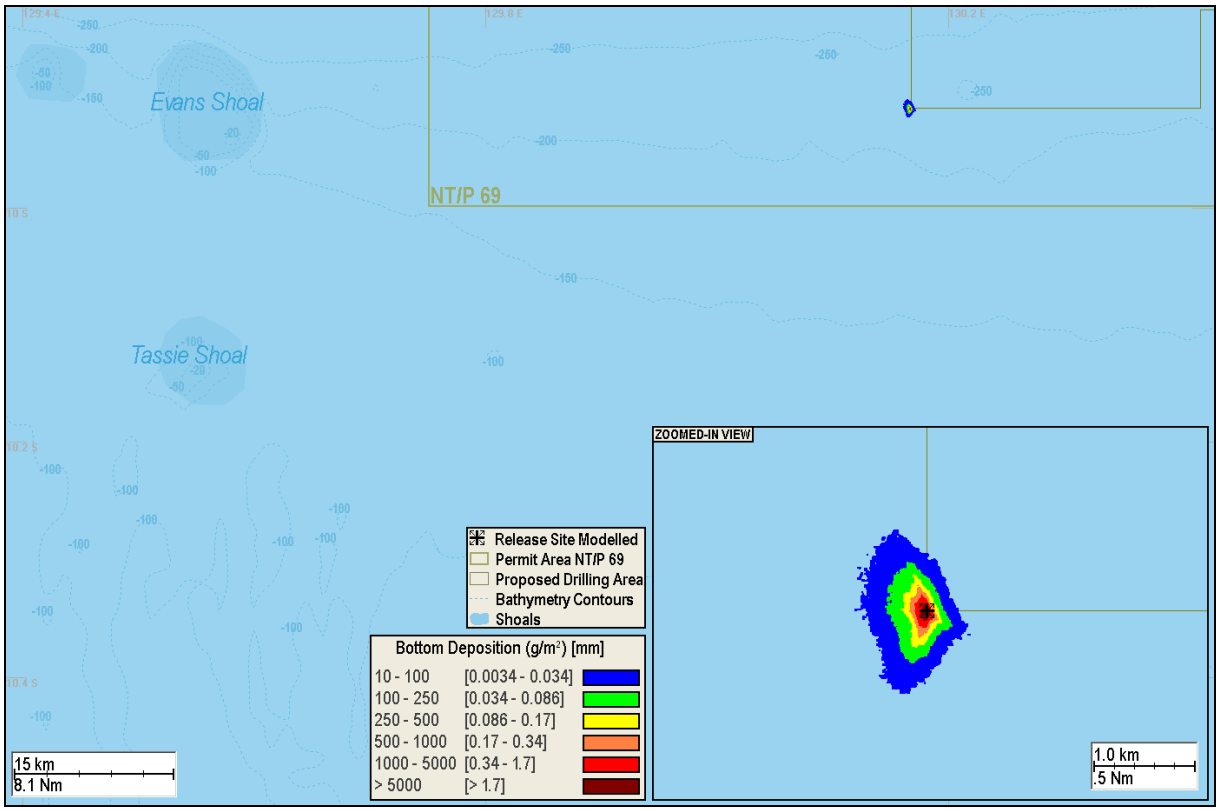

Figure 35: Predicted bottom deposition and seafloor coverage from the discharge of drill cuttings at the sea surface, commencing in November. The inset shows a zoomed in view.

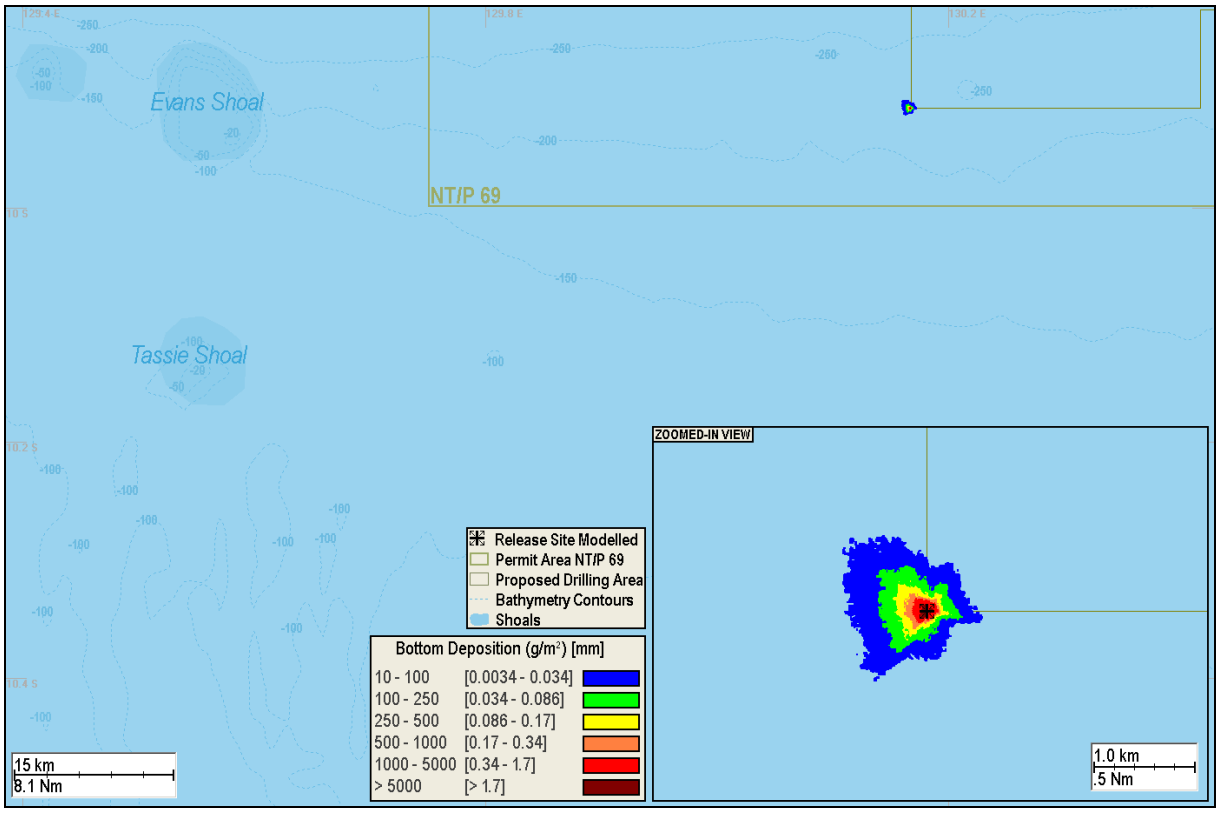

Figure 36: Predicted bottom deposition and seafloor coverage from the discharge of drill cuttings at the sea surface, commencing in December. The inset shows a zoomed in view.

5.4 Total Accumulated Thickness (Combined Discharges)

No contact was predicted (above a bottom deposition threshold of 10 g/m^2) for Evans Shoal and Tassie Shoal based on the combined seabed and surface discharge simulations at the release location for any of the 12 modelling commencement months. The predicted minimum distance from Evans Shoal and Tassie Shoal to the 10 g/m^2 contour was 53.1 km and 62.0 km, respectively.

Figure 37 to Figure 48 show the predicted bottom deposition (above 10 g/m^2) from the combined seabed and surface discharge simulations initiated at the start of each month (January to December).

Table 9 shows the predicted maximum seabed deposition and area of coverage (above 10 g/m^2) for the combined releases at the commencement of each month.

Figure 49 shows a cross section of the predicted thickness along the north-south and east-west axes by commencing discharges in November (based on the maximum predicted bottom thickness). The figure highlights the mounding adjacent to the discharge site and the exponential decline of the bottom thickness further away. Note the vertical axis is greatly exaggerated.

Table 9: Summary of the maximum predicted bottom thicknesses and area of coverage for the combined seabed and surface discharge simulations initiated on the first day of each month. Also shown is the minimum distance from sensitive receptors to the 10 g/m^2 contour.

Commencement month	***Maximum bottom deposition (mm)***	***Total area of coverage above the natural sedimentation threshold of 10 g/m^2 or 0.0026 mm (km^2)***	***Minimum distance from the sensitive receptor to the 10 g/m^2 contour (km)***	
			Evans Shoal	***Tassie Shoal***
January	400	1.66	60.6	68.1
February	362	11.43	60.4	68.0
March	429	4.28	58.5	66.4
April	391	12.41	53.1	62.0
May	377	13.85	59.8	67.8
June	401	11.83	53.2	62.1
July	392	19.12	55.6	65.4
August	431	6.88	56.8	65.4
September	375	14.87	59.0	67.2
October	416	13.29	54.9	65.2
November	437	6.44	58.0	66.0
December	397	10.84	58.5	67.5
Minimum	**362**	**1.66**	**53.1**	**62.0**
Maximum	**437**	**19.12**	**60.6**	**68.1**

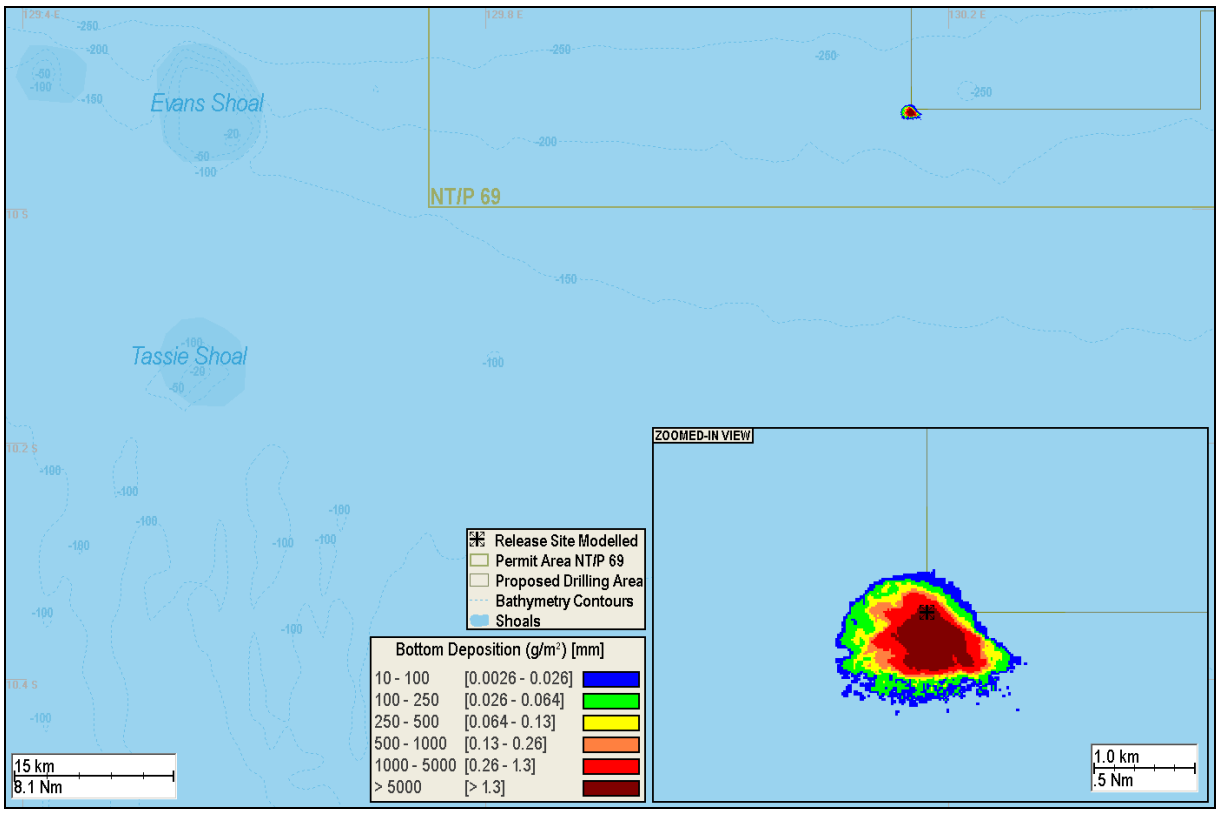

Figure 37: Predicted bottom deposition and seafloor coverage from the combined near-seabed and sea surface discharge simulations, commencing in January. The inset shows a zoomed in view.

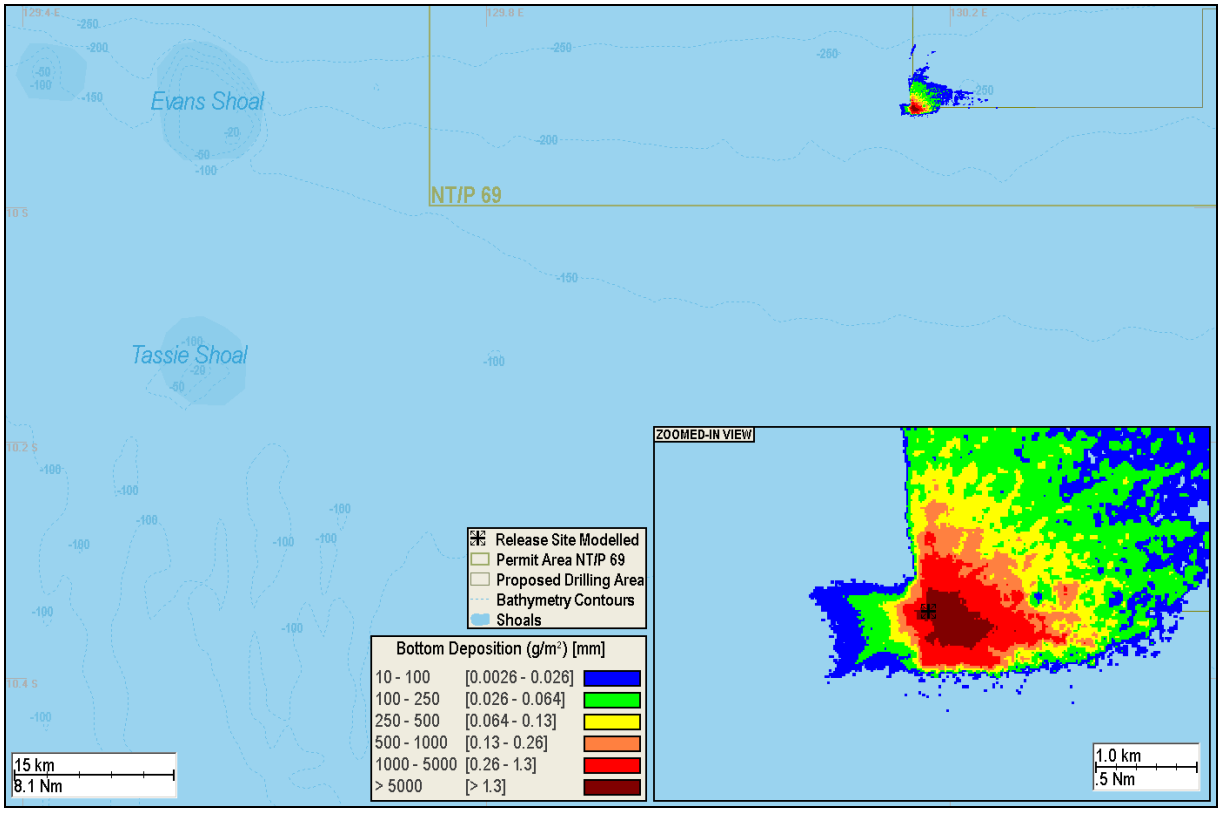

Figure 38: Predicted bottom deposition and seafloor coverage from the combined seabed and sea surface discharge simulations, commencing in February. The inset shows a zoomed in view.

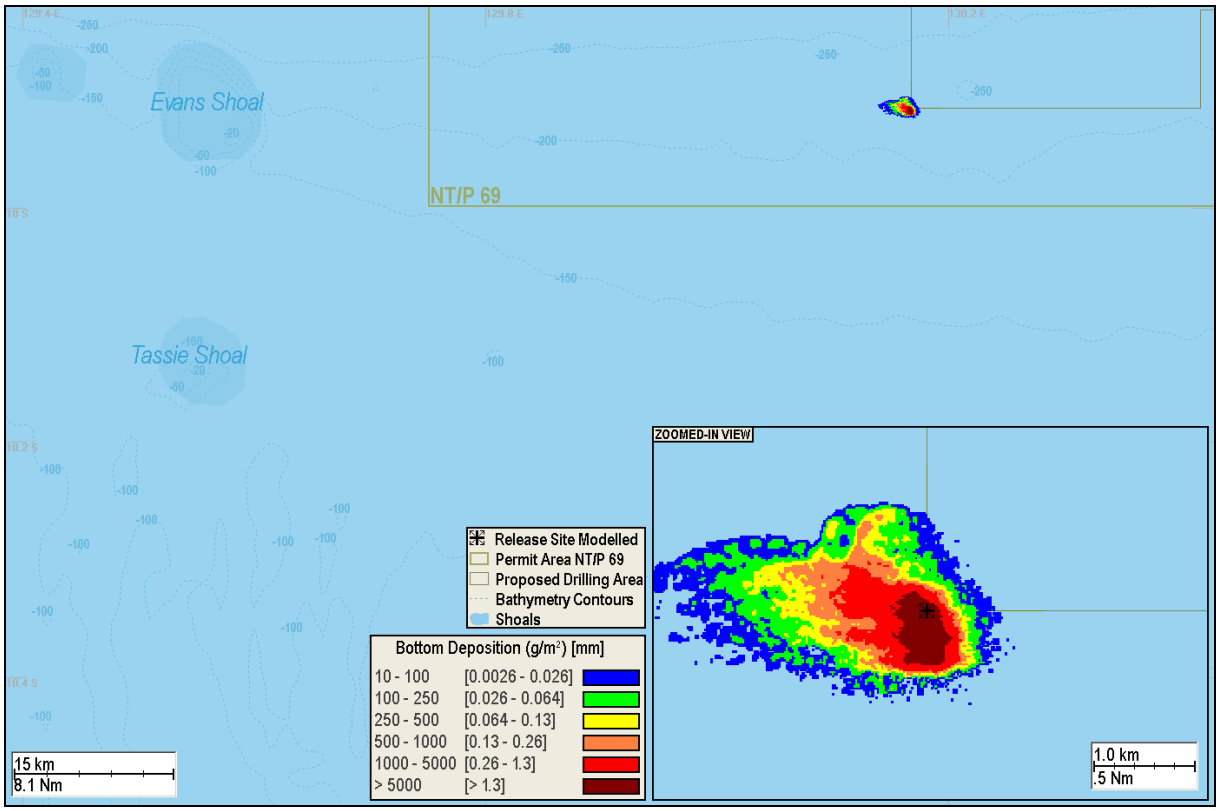

Figure 39: Predicted bottom deposition and seafloor coverage from the combined seabed and sea surface discharge simulations, commencing in March. The inset shows a zoomed in view.

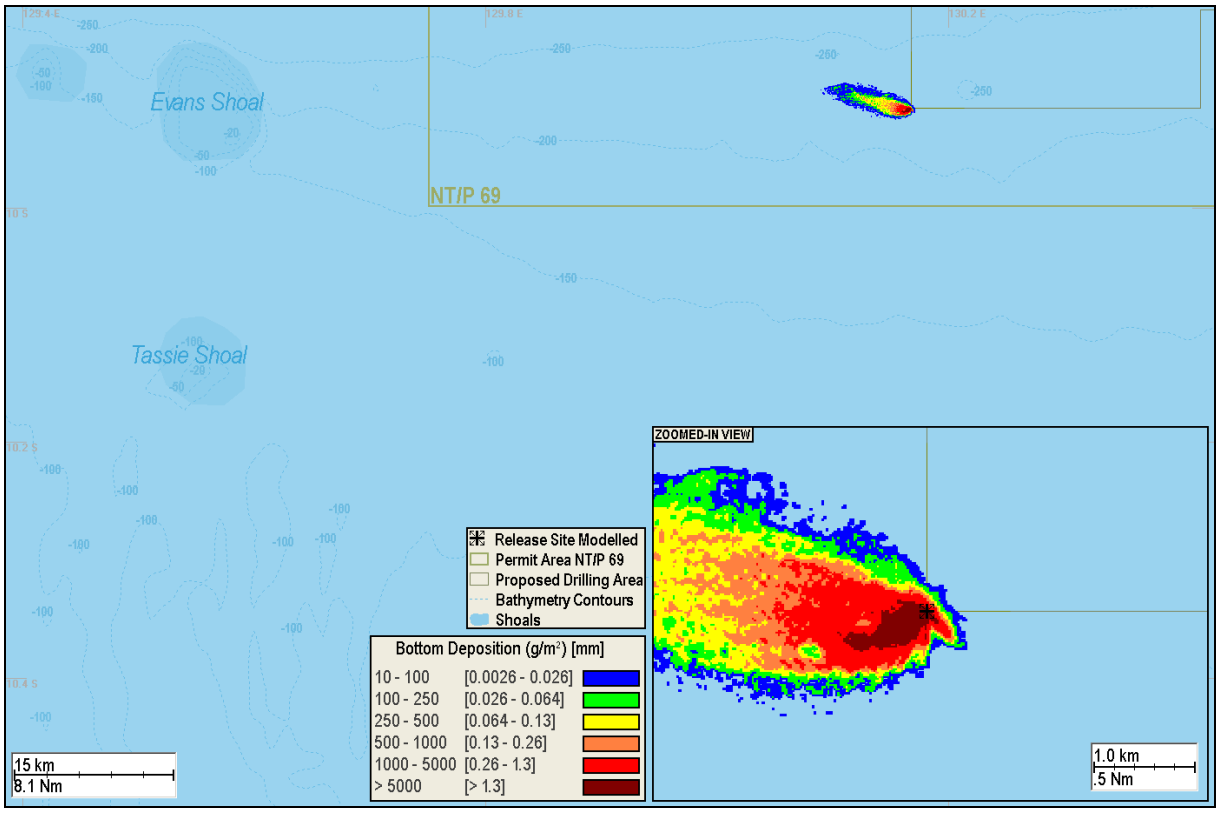

Figure 40: Predicted bottom deposition and seafloor coverage from the combined seabed and sea surface discharge simulations, commencing in April. The inset shows a zoomed in view.

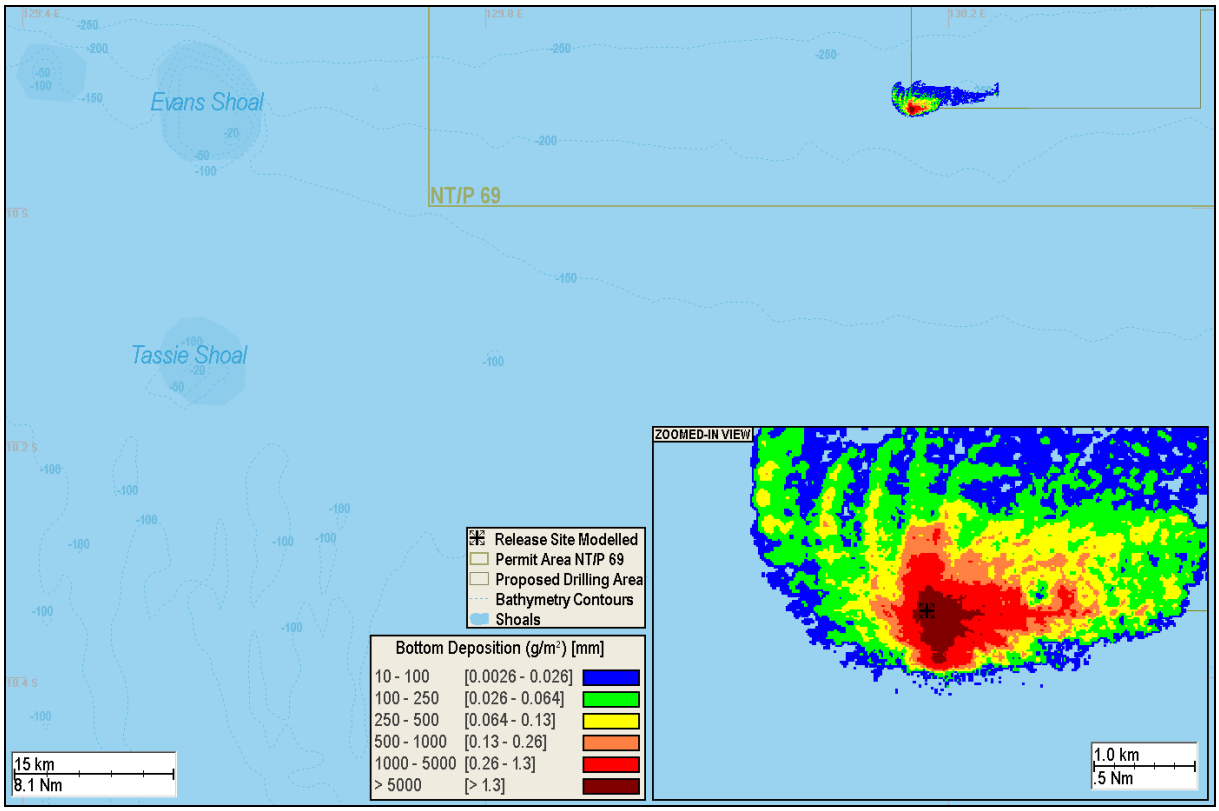

Figure 41: Predicted bottom deposition and seafloor coverage from the combined seabed and sea surface discharge simulations, commencing in May. The inset shows a zoomed in view.

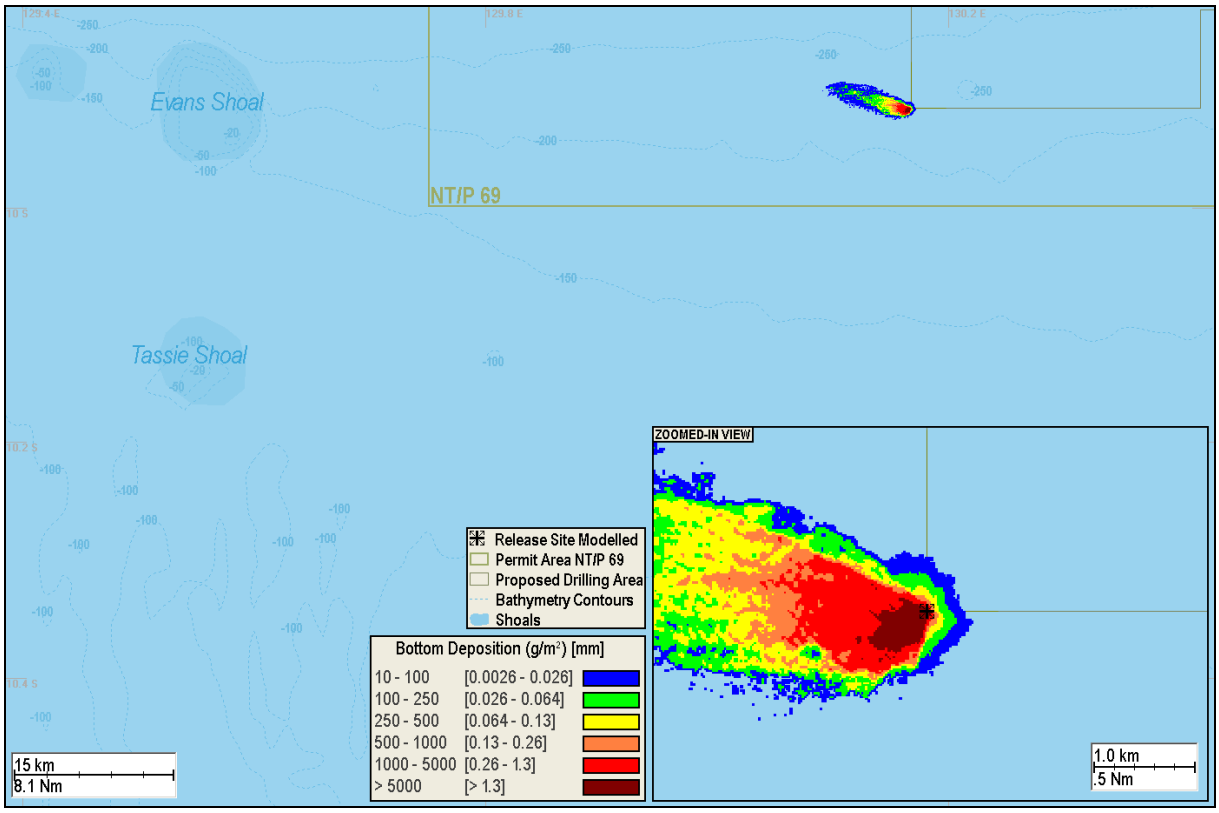

Figure 42: Predicted bottom deposition and seafloor coverage from the combined seabed and sea surface discharge simulations, commencing in June. The inset shows a zoomed in view.

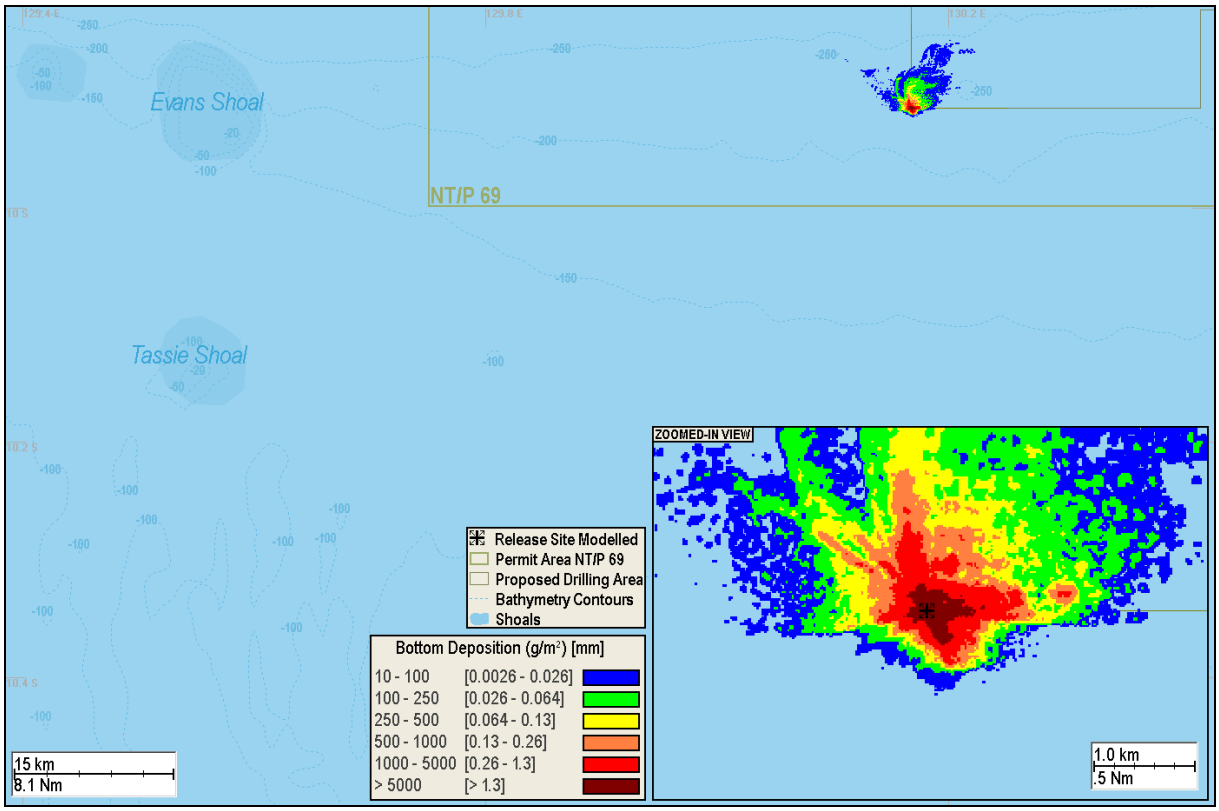

Figure 43: Predicted bottom deposition and seafloor coverage from the combined seabed and sea surface discharge simulations, commencing in July. The inset shows a zoomed in view.

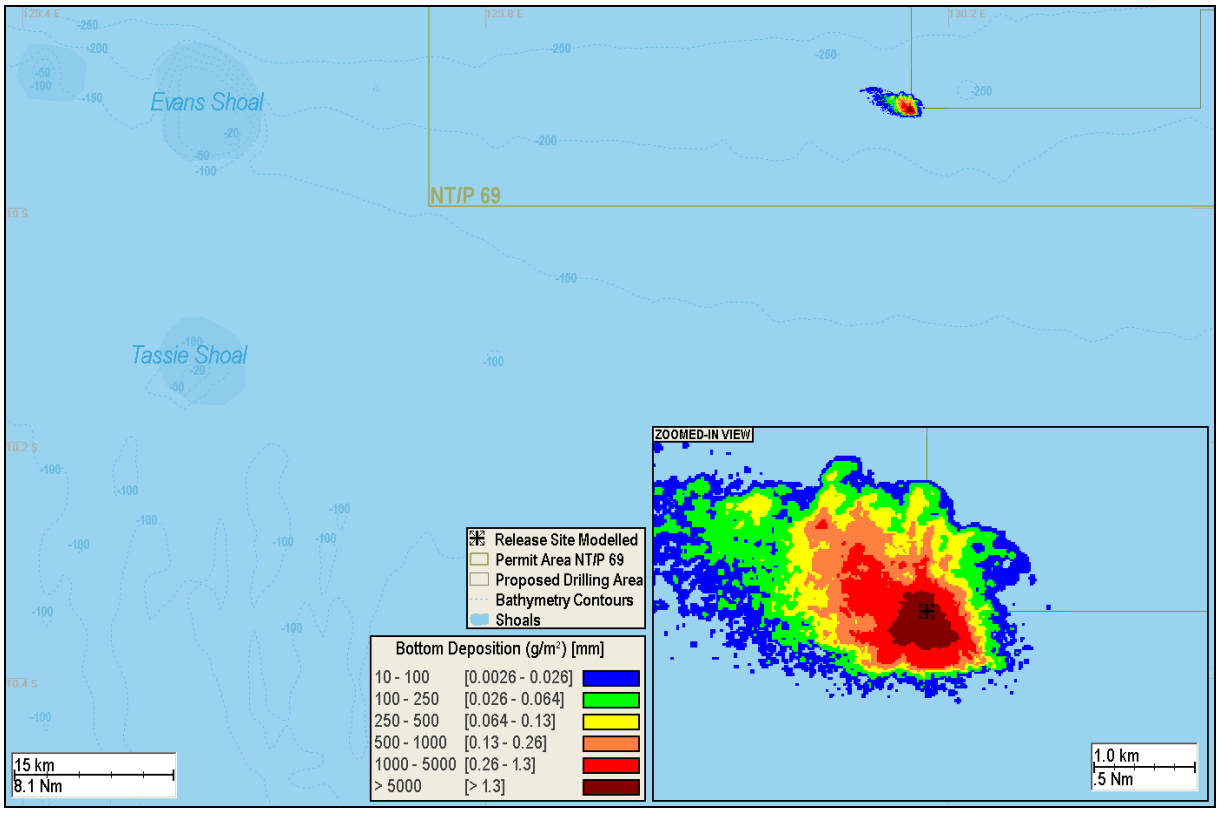

Figure 44: Predicted bottom deposition and seafloor coverage from the combined seabed and sea surface discharge simulations, commencing in August. The inset shows a zoomed in view.

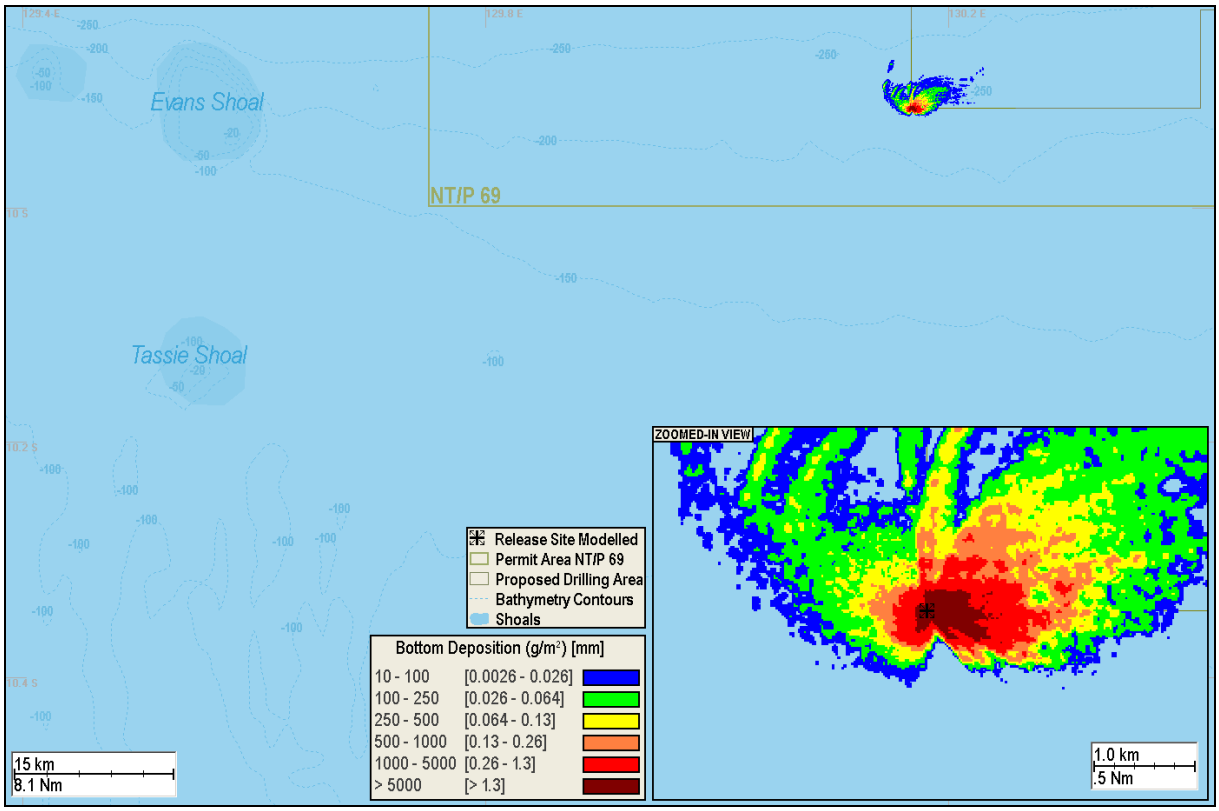

Figure 45: Predicted bottom deposition and seafloor coverage from the combined seabed and sea surface discharge simulations, commencing in September. The inset shows a zoomed in view.

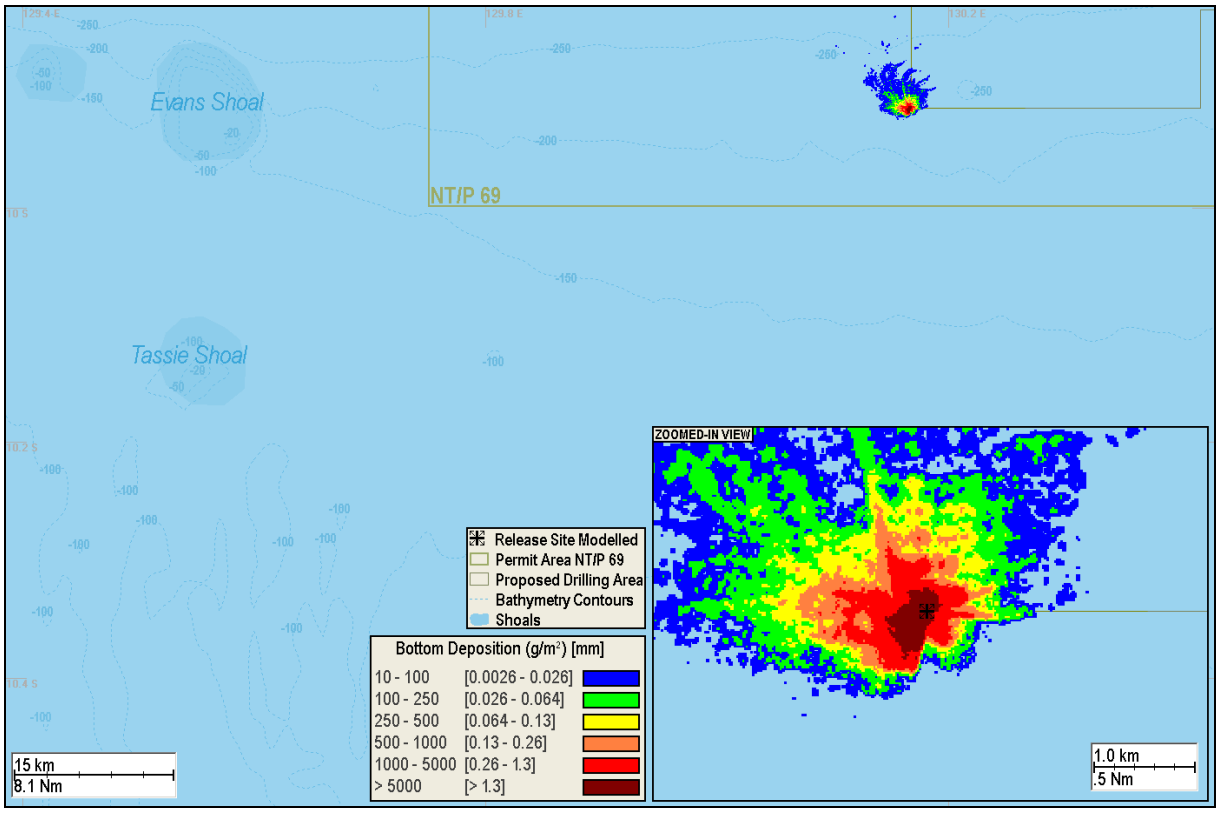

Figure 46: Predicted bottom deposition and seafloor coverage from the combined seabed and sea surface discharge simulations, commencing in October. The inset shows a zoomed in view.

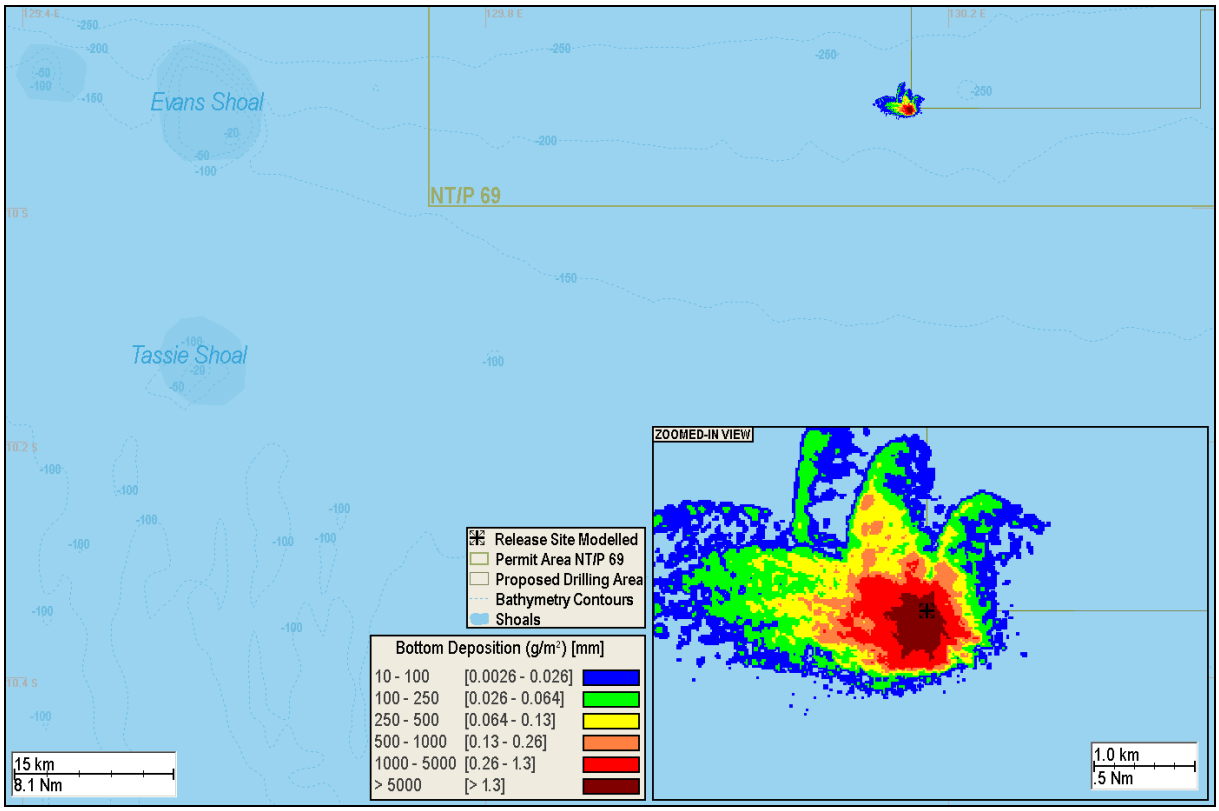

Figure 47: Predicted bottom deposition and seafloor coverage from the combined seabed and sea surface discharge simulations, commencing in November. The inset shows a zoomed in view.

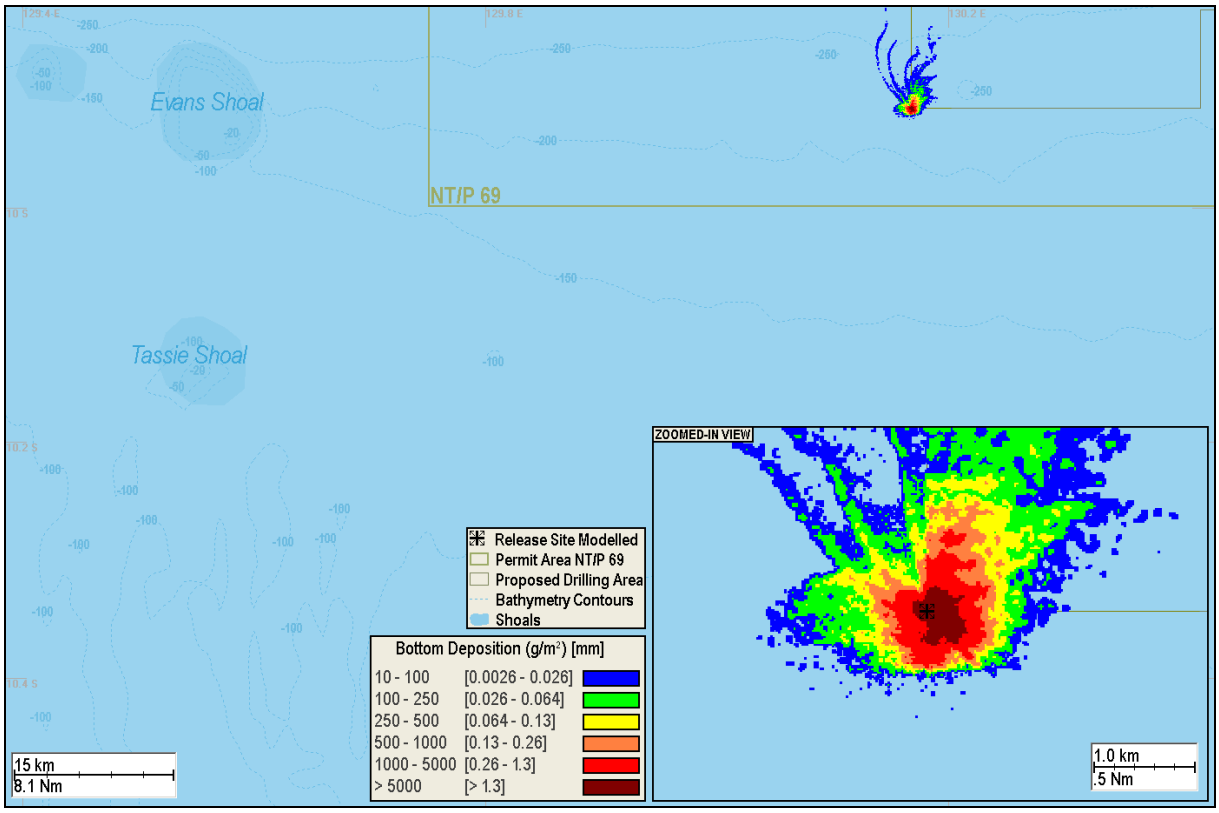

Figure 48: Predicted bottom deposition and seafloor coverage from the combined seabed and sea surface discharge simulations, commencing in December. The inset shows a zoomed in view.

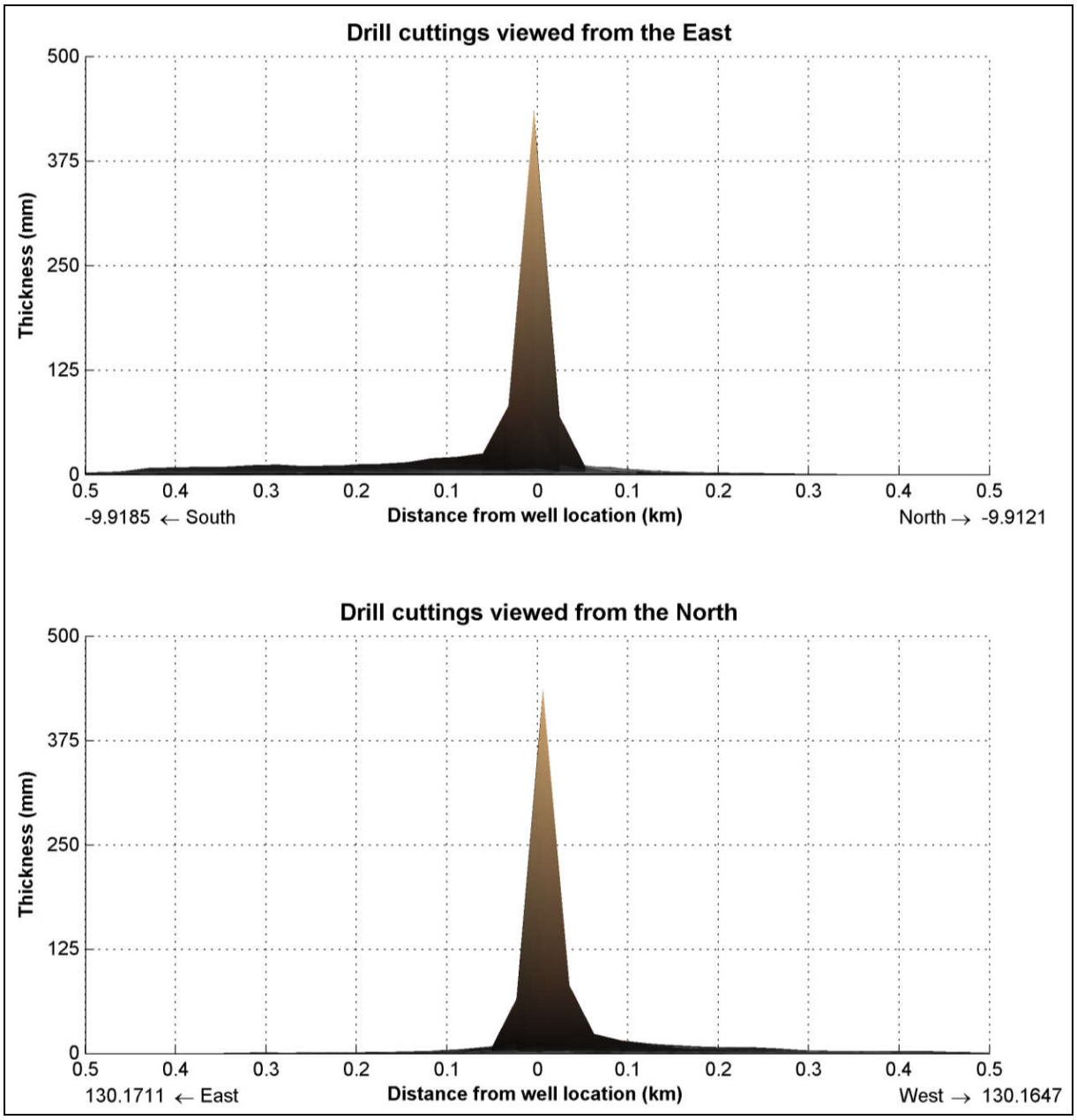

Figure 49: Cross sectional view of the predicted bottom thickness on the seafloor along the north-south axis (upper image) and east-west axis (lower image) from the combined seabed and sea surface discharge simulations. The images illustrate predicted bottom thicknesses corresponding to distances from the well in each cardinal direction. Results are based on the 39.3 day discharge of drill cuttings and muds commencing in November. Note the vertical scale is exaggerated.

6 REFERENCES

Geoscience Australia, 2009. *Australian Bathymetry and Topography Grid*. Australian Government Geoscience Australia.

Brandsma, M.G. and Sauer, T.C. Jr., 1983. *The OOC model: prediction of short term fate of drilling mud in the ocean, Part I model description and Part II model results.* Proceedings of Workshop on An Evaluation of Effluent Dispersion and Fate Models for OCS Platforms. Santa Barbara, California, 7th – 10th February, 1983.

Burns, K., Codi, S., Furnas, M., Heggie, D., Holdway, D., King, B. and McAllister, F., 1999. Dispersion and Fate of Produced Formation Water Constituents in an Australian Northwest Shelf Shallow Water Ecosystem. *Marine Pollution Bulletin 38,* 593–603.

Copeland, G., 1996. *UK Seminar on current research on data rich models of tidal flow and effluent dispersion*. University of Strathclyde, Department of Civil Engineering Report. Glasgow.

Davies, A. M., 1977a. The numerical solutions of the three-dimensional hydrodynamic equations using a B-spline representation of the vertical current profile. *Bottom Turbulence, Proceedings of the 8th Liege Colloquium on Ocean Hydrodynamics.* Nihoul, J.C. (Editor) Elsevier.

Davies, A.M., 1977b. Three-dimensional model with depth-varying eddy viscosity. *Bottom Turbulence. Bottom Turbulence, Proceedings of the 8th Liege Colloquium on Ocean Hydrodynamics*. Nihoul, J.C. (Editor) Elsevier.

Dyer, K.R., 1986. *Coastal and Estuarine Sediment Dynamics.* John Wiley & Sons, Chichester.

Foreman, M., Beauchemin, L., Cherniawsky, J., Pena, M., Cummins, P., and Sutherland. G., 2005. *A review of models in support of oil and gas exploration off the North Coast of British Columbia*. Canadian technical report of fisheries and aquatic sciences.

Gordon. R., 1982. *Wind driven circulation in Narragansett Bay*. PhD. Thesis. Department of Ocean Engineering, University of Rhode Island, Kingston, RI, 161 pp.

Isaji, T. and Spaulding, M., 1984. Notes and Correspondence. A Model of the Tidally Induced Residual Circulation in the Gulf of Maine and Georges Bank. *Journal of Physical Oceanography,* 1119–1126.

Isaji, T., Howlett, E., Dalton C., and Anderson, E., 2001. Stepwise-Continuous-Variable-Rectangular Grid. *Proceedings 24th Arctic and Marine Oil spill Program Technical Seminar,* 597–610.

King, B. and McAllister, F.A., 1997. *Modelling the Dispersion of Produced Water Discharge in Australia* 1 & 2. Australian Institute of Marine Science report to the APPEA and ERDC.

King, B. and McAllister, F.A., 1998. Modelling the dispersion of produced water discharges. *APPEA Journal*, 681–691.

Koh, R.C.Y. and Chang, Y.C., 1973. *Mathematical model for barged ocean disposal of waste. Environmental Protection Technology Series* EPA 660/2-73-029, U.S. Army Engineer Waterways Experiment Station. Vicksburg, Mississippi.

Khondaker, A.N. 2000. Modeling the fate of drilling waste in marine environment – an overview. *Journal of Computers and Geosciences* 26, 531–540.

Nedweed, T. 2004. Best practices for drill cuttings and mud discharge modelling. SPE 86699. Paper presented at the Seventh SPE International Conference on Health, Safety and Environment in Oil and Gas Exploration and Production, Calgary, Alberta, Canada. Society of Petroleum Engineers, P6.

Neff, J., 2005. Composition, environment fates, and biological effect of water based drilling fluids and cuttings discharged to the marine environment: A synthesis and annotated bibliography. Report prepared for Petroleum Environment Research Forum and American Petroleum Institute.

Oke, P.R., Brassington, G.B., Griffin, D.A., Schiller, A., 2008. The Bluelink ocean data assimilation system (BODAS). *Ocean Modelling* 21, 46-70.

Oke, P.R., Brassington, G.B., Griffin, D.A., Schiller, A., 2009. Data assimilation in the Australian Bluelink system. *Mercator Ocean Quarterly Newsletter* 34, 35-44.

Owen, A. 1980. A three-dimensional model of the Bristol Channel. *Journal of Physical Oceanography* 10, 1290–1302.

Schiller, A., Oke, P.R., Brassington, G., Entel, M., Fiedler, R., Griffin, D.A., Mansbridge J.V., 2008. Eddy-resolving ocean circulation in the Asian–Australian region inferred from an ocean reanalysis effort. *Progress in Oceanography* 76, 334-365.

Spaulding M.L., 1994. MUDMAP: A numerical model to predict drill fluid and produced water dispersion. Offshore, Houston Texas, March Issue.

Zigic, S., Zapata, M., Isaji, T., King, B., and Lemckert, C., 2003. Modelling of Moreton Bay using an ocean/coastal circulation model. *Coast and Ports Australasian Conference, 9th–12th September Auckland, New Zealand, paper 170*.